

EPSC2018
MTI3 abstracts

The Web-based Interactive Mars Analysis and Research System for the iMars project

Sebastian. H. G. Walter (1), Jan-Peter Muller (2), Panagiotis Sidiropoulos (2), Yu Tao (2), Klaus Gwinner (3), Alfiah R. D. Putri (2), Jung-Rack Kim (4), Ralf Steikert (1), Stephan van Gasselt (1,4), Greg G. Michael (1), Gillian Watson (2), Björn P. Schreiner (1)
 (1) Freie Universität Berlin, Germany (2) University College London, United Kingdom (3) German Aerospace Center (DLR), Germany (4) University of Seoul, South Korea (s.walter@fu-berlin.de)

Abstract

We describe the web-based interactive Mars Analysis and Research System (iMARS web-GIS), specialized on planetary surface change analysis with novel tools for simultaneous visualization of single images as time series in their original sequence. As the data foundation, we use the vast quantity of automatically co-registered ortho-images and digital terrain models (DTM) from three NASA missions' instruments processed and ingested in the context of the EU-funded iMars project [1]. The baseline for the co-registered images are the High Resolution Stereo Camera (HRSC) multi-orbit quadrangle image mosaics, which are based on bundle-block-adjusted multi-orbit DTM mosaics. Additionally we make use of the existing along-track bundle-adjusted HRSC single images and DTMs available at the planetary data archives. A web mapping application including the presented functionality has been implemented and is available at <http://imars.planet.fu-berlin.de> with the iMars project website (<http://www.i-mars.eu/web-gis>) serving as a mirror. The system has been built by using solely open source software, and the additional developments are publicly available.

1. Introduction

To achieve change detection visualization functionality for planetary application, we want to be able to display all co-registered images available from a certain spot on the surface in their full spatial resolution – and to show them together animated as a time series. In-depth analysis of the data requires functionality such as switching quickly between layers, known as flickering (in the case of two layers of images) or cycling (more than two layers).

2. Methods

The iMARS web-GIS comprises a browser-server infrastructure which loads dynamic code from a website and connects to web services of a server-based backend. The web services stream pre-processed data from connected databases and storage subsystems according to the standards of the OGC [2], adapted for planetary reference systems [3]. The iMARS web content (HTML, CSS) including dynamic code (JavaScript) is retrieved from a web server, gets executed in the browser and dynamically streams the topography, image and vector data from the server backends. Therefore we differentiate between the frontend and the backend of the system, with the stored web page on the server logically still belonging to the frontend side of the system, as it is interpreted on-the-fly and launched on the client (Fig. 1). The client code consists of the map canvas with user interface components, including attribute filter masks and data layer selection components. The selected data layers are requested directly from the map cache instance via concurrent OGC-based Web Map Service (WMS) and Web Feature Service (WFS) calls.

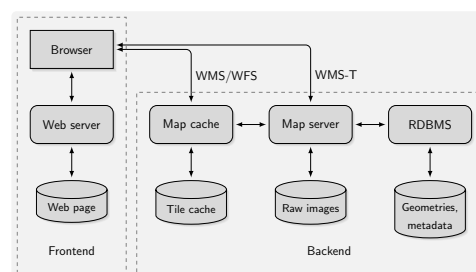


Figure 1: System design of the iMARS web-GIS outlining frontend (client) and backend (server) components.

Due to the vast number of single images we needed a way to set up the layers in a dynamic way since the map server does not know the images to be served beforehand. This requires an additional parameter associated with the PDS product ID (a unique identifier available for all NASA and ESA mission data products). In the OGC definition, such non-standard parameters providing enhanced capabilities can be realized as vendor-specific parameters (VSP) [2]. To provide dynamic layers, we introduce the `PRODUCTID` parameter in the WMS request to the map server. To ensure compatibility with regular WMS, the service will produce a valid result using a predefined default if the `PRODUCTID` parameter is omitted or malformed.

The dynamic service is implemented as a *MapScript* instance of MapServer. MapScript connects the Apache web server to the MapServer application programming interface (API) using CGI and provides an interface for the Python language. When used in the context of OGC services, it is capable of intercepting the request and using the request parameters for further processing. We use internal map template configurations with incomplete file paths for each available dynamic layer representing a camera instrument. With the product ID provided as an additional parameter, the internal path to the requested image on disk is constructed and the map is then finally configured. In this way, the individual layers are created on-the-fly, each representing only one single image. On the frontend side, the VSP request parameter (`PRODUCTID`) has to be appended to the regular set of WMS parameters. The pool of available product IDs is constructed from the requested attributes of the footprint coverage query on the frontend. Therefore, a coverage query always has to precede the single image query and visualization.

For external data queries and access, we have successfully extended the dynamic WMS services and implemented the Europlanet Data Model Table Access Protocol (EPN-TAP) [4] to provide Virtual Observatory (VO) access to the single HRSC "granules" via WMS [5]. As a first step, the single HRSC Level-3 images are available in Equidistant Cylindrical projection and can be queried by attribute keywords or geometry. Therefore the Python scripts have been extended to produce dynamic `GetCapabilities` output with available images as individual layers.

3. Frontend

The frontend is based on the *OpenLayers* JavaScript library. We have created special interface elements,

such as the *Time panel* for temporal filtering and the ortho-image *Workflow toolbar* for visualizing single images. All available data produced from within the iMars project have been included together with other available data sets useful for providing additional context. Navigation is provided by an interactive pan-, zoom- and click environment common to all user interface elements placed on the actual map canvas (see Fig. 2).

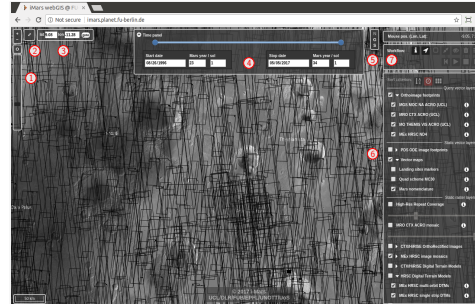


Figure 2: Browser view of the iMARS web-GIS with the user interface controls shown (numbered in red); 1: Zoom controls; 2: Fullscreen control; 3: Goto lat,lon; 4: Time panel; 5: Projection switcher; 6: Layer switcher; 7: Workflow toolbar.

Acknowledgements

This research has received funding from the EU's FP7 Programme under iMars 607379 and by DLR Bonn, grant 50QM1702. The project has made use of the USGS ISIS3. The software developed in the context of the iMARS web-GIS project is available at <https://github.com/imars-fub>.

References

- [1] Muller, J.-P., et al. (2016), *ISPRS Archives, XLI-B4*, 453–458.
- [2] Open Geospatial Consortium (2002), *Web Map Service Implementation Specification*.
- [3] Hare, T. M., et al. (2018), *PSS 150*, 36–42.
- [4] Erard, S., et al. (2014), *Astronomy and Computing* 7-8, 52–61.
- [5] Minin, M., et al. (2016), *AGU 31*, p. 1759.

SPICE for ESA Planetary Missions: geometry and visualization support to studies, operations and data analysis

M. Costa

European Space Agency, ESAC – ESA SPICE Service, Cross Mission Support Office, Spain, (marc.costa@esa.int)

Abstract

SPICE is an information system that provides the geometry needed to plan scientific observations and to analyze the obtained. The ESA SPICE Service generates the SPICE Kernel datasets for missions in all the active ESA Planetary Missions. This contribution describes the current status of the datasets, the extended services and the SPICE support provided to the ESA Planetary Missions (Mars Express, ExoMars2016, ExoMars2020, Solar Orbiter, BepiColombo, JUICE, Rosetta, Venus Express and SMART-1) for the benefit of the science community.

1. Introduction

SPICE is an information system the purpose of which is to provide scientists the observation geometry needed to plan scientific observations and to analyze the data returned from those observations. SPICE is comprised of a suite of data files, usually called kernels, and software -mostly subroutines [1]. A customer incorporates a few of the subroutines into his/her own program that is built to read SPICE data and compute needed geometry parameters for whatever task is at hand. Examples of the geometry parameters typically computed are range or altitude, latitude and longitude, phase, incidence and emission angles, instrument pointing calculations, and reference frame and coordinate system conversions. SPICE is also very adept at time conversions.

2. SPICE for ESA Missions

ESA has a number of science missions under development and in operations dedicated to the study of our Solar System (Mars Express, Rosetta, ExoMars, BepiColombo, Solar Orbiter and JUICE). The Science Operations Centers for these missions, located at the European Space Astronomy Centre (ESAC) in Spain, are responsible for all science

operations planning, and archiving tasks, being the essential interface between the science instruments who process these data, and the spacecraft via the Mission Operations Center located at the European Space Operations Center (ESOC) in Germany, and with the scientific community. From the concept study phase to the day-to-day science operations, these missions produce and use auxiliary data (spacecraft orbital state information, attitude, event information and relevant spacecraft housekeeping data) to assist science planning, data processing, analysis and archiving. Auxiliary data are those that help scientists and engineers to determine the location and orientation of the spacecraft, when and how an instrument was acquiring scientific data. These data also help to determine what other relevant events were occurring on the spacecraft or ground that might affect the interpretation of the scientific observation or the S/C systems performance. Software applications are required to know what were the location, size, shape and orientation of the observed target in addition to these auxiliary data. All ESA planetary missions have embraced the use of the SPICE system for ancillary data archiving and for science data analysis. Although the Flight Dynamics Division provides software to read the position and orientation files of the orbiters, most of the Principal Investigators have pointed out their interest in having all the auxiliary data distributed in SPICE format.

3. The ESA SPICE Service

The ESA SPICE Service (ESS)¹ located at ESAC leads the SPICE operations for ESA missions. The group generates the SKDs for missions in operations (EM16, MEX) missions in development (SOLO, BepiC, JUICE and ExoMars 2020) and legacy missions (ROS, VEX, SMART-1, Huygens and Giotto). The generation of these datasets includes the operational software pipelines to convert orbit,

¹ <http://spice.esac.esa.int>

attitude, telemetry and spacecraft clock correlation data into the corresponding SPICE format. ESS also provides consultancy and support to the Science Ground Segments of the planetary missions, the Instrument Teams and the science community. ESS works in partnership with NAIF and with the SPICE support for IKI/ROSCOSMOS. Finally, ESS periodically organizes training classes and workshops.

The current status of the SKDs for the before mentioned missions –most of which are publicly available- and the resources available to use that data and exploit are described in the following sections. The ESS reviews the legacy and operational datasets and develops the ones for the future missions, -the MEX and VEX SKDs are currently under review whereas the EM16, ROS, BepiC, Solar Orbiter and JUICE SKDs are in an optimal state according to their applicability. ESS is also responsible for generation of PDS3 and PDS4 formatted SPICE Archives that are published by the Planetary Science Archive of the European Space Agency (PSA) [2]. ESS, in close collaboration with NAIF peer-reviews the operational kernels for the PSA to publish being compliant with the Planetary Data System (PDS) standards and uses them in the processes that require geometry computations.

4. SPICE Kernel Datasets

The main purpose of the ESS is to provide a complete, consistent, high-quality, validated and up-to-date SKDs for the mission it supports in order to be able to use SPICE in an operations environment and for data analysis. A SKD consists on a complete set of SPICE Kernels that cover the whole mission lifespan including predicted long term, operational and reconstructed and or “measured” trajectory and orientation information. Kernels in a SKD can be classified in two main types:

Setup Kernels (STK) they are typically text files and they are developed by ESS and are reviewed and iterated with the SGS and with the Instrument Teams when need be during the whole duration of the mission. The STKs include the following information:

- Set of Reference Frames of interest for geometry computations.
- FoV and boresight modeling for science payload.
- Study trajectory default orientation for S/C.

- Physical models for natural bodies of the mission.
- Digital shape models for S/C elements.

Time-Varying Kernels (TVK) [SPK, CK, SCLK, MK] are either text or binary files and are generated with an auxiliary data processing pipeline and the source auxiliary data is provided by the Flight Dynamics team (FDy). TVKs include the following information:

- Predicted attitude and predicted/reconstructed trajectory.
- OBT to UTC/CAL time conversion.
- Reconstructed trajectory and measured orientation for S/C.
- Orientation of Solar Arrays, HGA, MGA or any other moving element of the S/C.
- Position of scans or turn-tables or articulations of payload.
- Digital Shape models for local terrain or extended bodies shapes

In addition to the two types of kernels included the SKD, SKDs can be classified in one of the following states depending on the mission phase they are:

Studies or pre-operational (JUICE, BepiC, SOLO and ExoMars 2020): These kernel datasets are characterized for being highly dynamic with changes in Instrument and S/C frames definitions. Usually different study cases for different consolidated trajectories provided by Mission Analysis (MAN) and with default and or study S/C Orientations are generated by the ESS.

Operational (MEX, EM16): These kernel datasets are updated with kernels generated from the periodical trajectory and orientation updates and from the relevant information obtained from housekeeping telemetry. Some updates on Instrument and S/C models might occur responding to operational demands (e.g.: after commissioning, after the start of the science phase, due to some particular event, etc.)

Legacy or post-operational (ROS, VEX): These ought to be final peer-reviewed and consolidated datasets. This process is currently on-going for both missions. The generation of the SKDs for Giotto and Huygens has not begun yet.

SKDs are released in a regular basis with STKs-lead updates, for missions in operations this also includes periodical updates to ensure that the latest data is available with the automatic generation of TVKs. SKDs are properly documented with general descriptions, status reports, “readme” files per kernel type and release notes.

4.1 Kernels Generation an Update

Whilst the generation of STKs does not require further explanation on their generation, TVK kernels; S/C trajectory, attitude and SC components orientation kernels do. Typically, a SKD will contain the following pieces of information:

1. Set of Reference Frames of interest for geometry computations (FK).
2. FoV and boresight modeling for remote and in situ sensors -at least- (IK)
3. Predicted trajectory and as-planned or default orientation for the S/C (SPK, CK)
4. OBT to UTC/CAL time conversion (SCLK)
5. Reconstructed trajectory and orientation and on-board measured orientation for S/C
6. Orientation of S/C parts (CK from HK Telemetry)
7. Position of scans or turn-tables or articulations of payload (CK from HK Telemetry)

Both 1. and 2. kernels will be ready already for the study phase and will be generated by ESS, whilst 3. will be hardly updated during the study phase but will be periodically generated during the science phase. From 3. to 7., those kernels will be generated by an operational pipeline. The particular order in which they have been described indicates how important are they for users and which implementation priority they do have. For instance, although all of them are implemented for MEX.

4.2 Kernel Dataset Distribution

Most of the SKDs for ESA Missions are publicly available² (hence the “at your glance” part of the title

² ROS, MEX, VEX, SMART-1, Chandrayaan-1, EM16, BepiC and JUICE are publicly available for ultimately ESS is responsible for these data. For SOLO the SGS is responsible for its distribution and although ultimately they will be made public, the current study SKD is not. ExoMars 2020 is a special

of this contribution) and all the relevant information on how to obtain and use the available SDKs can be found in the home page for SPICE at ESA³. Public SKDs are distributed to the users by three different means:

File Transfer Protocol (FTP): The FTP⁴ contains all the kernels that have been generated for any mission and it also contains the operational MK that specifies which are the latest applicable kernels. This might not be the best solution for users to obtain a SKD for they need third party applications to manage the SKD or they need to obtain the kernels manually. This FTP is mirrored by NAIF for most of the missions.

Zippered directory. There is a permanent link to the latest SKD, containing only a subset of the kernels present in the latest operational meta-kernel. This solution is recommended for a user that need to make quick usage of the latest SKD.

Git repository. Distribution of SPICE Kernel Dataset via Git is available in BitBucket⁵ and the latest version of a subset of the SKD for a given meta-kernel will be available via a Git Pull. Large files (SPKs and CKs mainly) are available without overloading the repository with GIT-lfs (GIT large file system). This is considered to be the best solution to work with SPICE Kernels.

Please note that as already indicated the SPICE FTP contains all the kernels that have ever been generated and published for a given mission; a user can always reproduce a given mission scenario for any mission period.

5. Using SPICE for ESA Planetary Missions

The ESS offers other services beyond the SPICE Kernels datasets, such as configuration and instances for WebGeocalc and Cosmographia for the ESA Missions [3].

case for ESS collaborates and provides consultancy to the ExoMars 2020 Rover and Surface Platform Operations Centers but is not ultimately responsible for the SPICE data.

³ <https://www.cosmos.esa.int/web/spice/data>

⁴ <ftp://spiftp.esac.esa.int/data/SPICE>

⁵ https://repos.cosmos.esa.int/socci/projects/SPICE_KERNELS

5.1 SPICE-Enhanced Cosmographia

SPICE-enhanced Cosmographia (COSMO) [4] is an interactive tool used to produce 3D visualizations of planet ephemerides, sizes and shapes; spacecraft trajectories and orientations; and instrument field-of-views (FoV) and footprints. COSMO is provided by NAIF and is based on the well-known 3D visualization tool Celestia. It can also be used to display simple geometrical quantities such as angles of separation in between given directions and distances. These characteristics make Cosmographia an ideal complementary tool for planning an instrument pointing profile, observation geometry visualization and evaluation of a planned trajectory (it is also very useful for PR purposes).

COSMO needs the generation of a set of input files – JSON configuration files- which are generated by ESS and are publicly available for most of the ESA Planetary missions⁶.

5.2 WebGeocalc

The main drawback of using SPICE is that it usually requires a user which has moderate programming skills along with a reasonable experience with the data and geometry of the mission that she/he is going to work on. An excellent workaround for this drawback is WebGeocalc (WGC) [4]. WGC provides a web-based graphical user interface to many of the observation geometry computations available from SPICE. A WGC user can perform SPICE computations without the need to write a program; the user needs to have only a computer with a standard web browser. WGC can support ESA's planetary projects and planetary data research in several ways:

- It opens up much of the SPICE computational capability to those unable to write programs.
- It offers a mechanism that scientists and engineers may use to help verify their own SPICE-based code.
- It provides a quick and easy means for peer reviewers of science data archives to spot check many of the observation geometry computations included in the archive.
- It opens the possibility to obtain a quick answer to a geometry question arising during a meeting.

⁶

<https://www.cosmos.esa.int/web/spice/cosmographia>

WGC makes the job of computing many kinds of observation geometry quicker and somewhat easier than if one has to write a program to do so. With this characteristics WGC is ideal both for missions in operations in order to quickly assess the feasibility of observations in terms of derived quantities and – specially- for missions in development. A WGC instance for ESA Planetary missions is available⁷. This instance includes operational, archived, study, test and SPICE lessons scenarios and complements the NASA instance which is available in the NAIF server.

5.3 An example use case for data analysis

Let's take it from the data analysis perspective. Say that we are working with Mars-Express data, more concretely we are performing surface studies of Phobos, the Martian moon. First of all, we can access the PSA web-based user interface [2]⁸ and retrieve the list of Phobos observations by the High Resolution Stereo Camera (HRSC) on board of MEX. We would like to somehow constrain our search by only looking for those who provide us a good resolution, namely; those which were acquired at a distance closer than 1.000 km. How can we constrain our search? One option would be to check the PDS3 labels of all the images and look for that geometrical information, which will definitively be an arduous task, or, we could use SPICE. Say that, on top of this we want to know the illumination of a given set of surface areas and we also want to know the intersection of the instantaneous FOV (iFOV) of a given pixel of the HRSC sensor. We will certainly not find that geometry information anywhere in the archive: SPICE is the solution.

But, in all those SPICE use cases mentioned in the paragraph before, how could we proceed? Well to begin with we could immediately use an Application Programming Interface (API) of the the Geometry Finder (GF) subsystem available with WGC that allows us to find time windows for which a given geometry condition is met (the inverse problem of calculating a given quantity of interest), see Fig.1. That would give us a list of time windows with the periods in which MEX was less than 1.000 km from Phobos and then we could use those time windows in the PSA UI to constrain the Phobos image search

⁷ <http://spice.esac.esa.int/webgeocalc/>

⁸ <https://archives.esac.esa.int/psa>

(see Fig.2). Say we decide to go with the image in Fig.3). What we could do next in order to better understand the observation geometry is to run the COSMO scenario with the MEX kernels, with that we could obtain the context depicted in Fig.4 and Fig.5, and as can be seen in Fig.6, we could also use the HRSC boresight and FoV and obtain a simulation of the image itself. The geometry seems alright and there is a very good match with the real data. Now, in order to obtain the illumination of a given surface location on Phobos, we could write a SPICE-based script/function in one of the languages that SPICE is available for (C, FORTRAN, Matlab, IDL or Python).

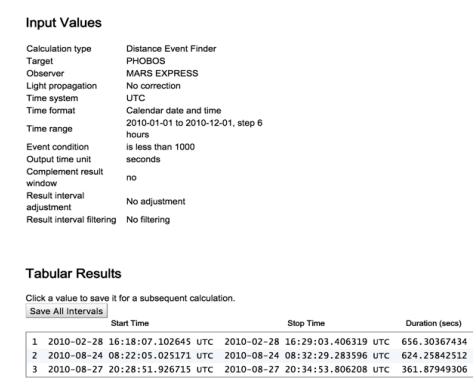


Figure 1: Result window of WebGeocalc.

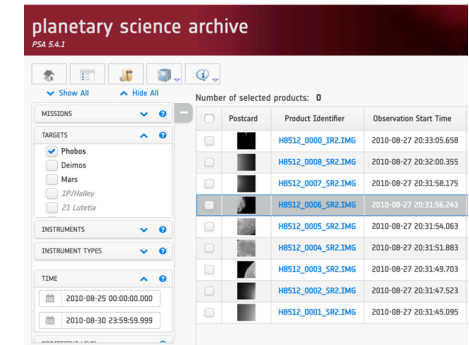


Figure 2: PSA web UI with a search for Phobos.

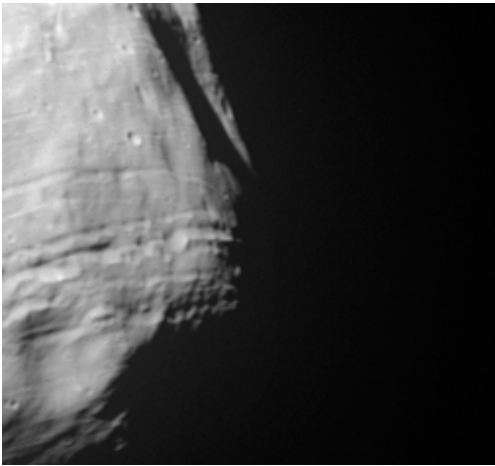


Figure 3: HRSC image of Phobos

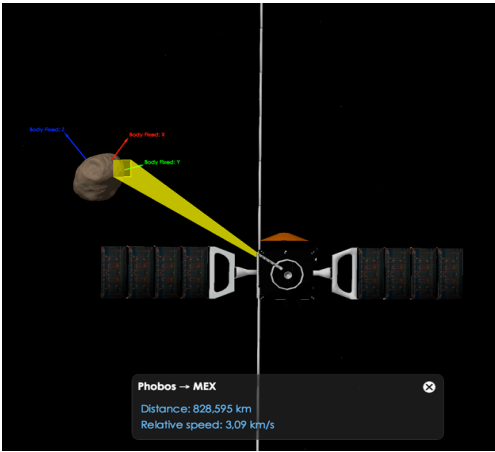


Figure 4: SPICE-enhanced Cosmographia with MEX HRSC Phobos observation.

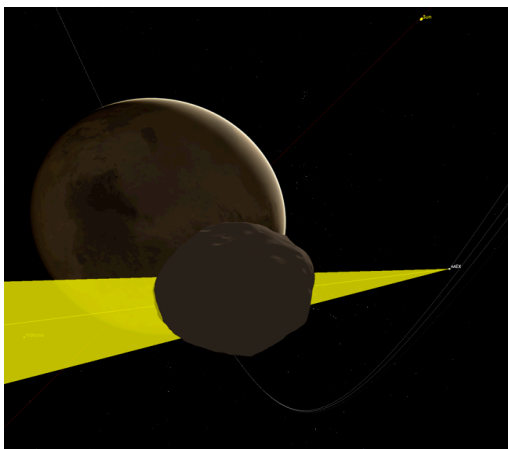


Figure 5: SPICE-enhanced Cosmographia MEX
HRSC Phobos observation context.

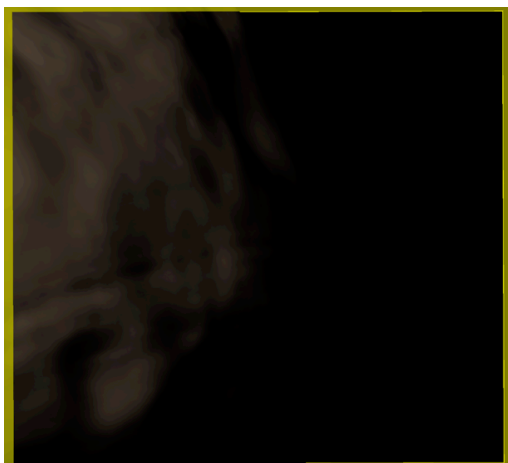


Figure 5: SPICE-enhanced Cosmographia MEX
HRSC Phobos observation FOV view.

References

- [1] Acton C., Ancillary data services of NASA's Navigation and Ancillary Information Facility (1996), Planet. And Space Sci., 44, 65-70.
- [2] Bessel, S. et al., ESA's Planetary Science Archive: Preserve and Present Reliable Scientific Datasets (2018) Planet. And Space Sci., 150, 131-140.
- [3] Acton, C. et al., A Look Towards the Future in the Handling of Space Science Mission Geometry (2018) Planet. And Space Sci., 150, 9-12.

SPICE-based Python packages for Solar System Exploration geometry exploitation

M. Costa (1), M. Grass (2)

(1) European Space Agency, ESAC – ESA SPICE Service, Cross Mission Support Office, Spain, (marc.costa@esa.int)

(2) IRS, University of Stuttgart, Pfaffenwaldring 29, 70569 Stuttgart, Germany, (mgrass@irs.uni-stuttgart.de)

Abstract

SPICE is an information system that provides the geometry needed to plan scientific observations and to analyze the obtained. The ESA SPICE Service generates the SPICE Kernel datasets for missions in all the active ESA Planetary Missions. Sometimes it is hard to find a particular functionality that a user or a group might require and it is not uncommon that users need to develop their own functions with a given combination of SPICE APIs, at ESA we have identified a set of functions and wrapped them up in a series of Python packages along with other features that improve the user experience with SPICE. This contribution provides an overview of those packages.

1. Introduction

SPICE is an information system the purpose of which is to provide scientists the observation geometry needed to plan scientific observations and to analyze the data returned from those observations. SPICE is comprised of a suite of data files, usually called kernels, and software -mostly subroutines [1]. A customer incorporates a few of the subroutines into his/her own program that is built to read SPICE data and compute needed geometry parameters for whatever task is at hand. Examples of the geometry parameters typically computed are range or altitude, latitude and longitude, phase, incidence and emission angles, instrument pointing calculations, and reference frame and coordinate system conversions. SPICE is also very adept at time conversions.

2. SPICE for ESA Missions

The ESA SPICE Service (ESS) leads the SPICE operations for ESA missions. ESS generates the SPICE Kernel Datasets (SKDs) for missions in operations (ExoMars 2016, Mars Express) missions in development (BepiColombo, JUICE) and legacy

missions (Rosetta, Venus Express). ESS is also responsible for the generation of SPICE Kernels for Solar Orbiter. The generation of SKDs includes the operation software to convert ESA orbit, attitude, payload telemetry and spacecraft clock correlation data into the corresponding SPICE format. ESS also provides consultancy and support to the Science Ground Segments of the planetary missions, the Instrument Teams and the science community. ESS works in partnership with NAIF [2]. In addition to the services described in the previous section, ESS is developing several services in the shape of Python packages to enhance the exploitation of SPICE data.

3. spiops a Python package for SPICE

spiops is a Python package that uses SpicePy¹ (a Python wrapper for the C implementation of SPICE) to use SPICE Toolkit APIs in order to provide higher-level functions than the ones available with SPICE. spiops is aimed to assist the users to extend the usage of SPICE. These functions have been identified in the day-to-day work of the ESS and its clients from having to implement multiple times a series of SPICE APIs to obtain a given derived functionality which is not directly available as a SPICE API. Functionalities vary from the computation of the illumination of a given FoV to obtaining the coverage of a given S/C for a particular MK, plotting Euler Angles or comparing different kernels. All that providing integrated plotting capabilities as well. In general, by design spiops offers three different types of functions:

1. SPICE based derived functions,
2. non-SPICE based derived functions and
3. an object Oriented SPICE interface

The underlying idea of spiops is to be used as a multi-user and multi-disciplinary pool of re-usable SPICE based functions and to provide an easier interface to

¹ <https://github.com/AndrewAnnex/SpiceyPy>

certain SPICE functionalities with objects to provide cross mission and discipline support of SPICE for ESA Planetary and Heliophysics missions. The ultimate goal is to provide:

1. A Pool for functions that ESS uses needed to work with SPICE,
2. an Interface to provide solutions to users, a Library for SPICE-based applications.

spiops is publicly available as a Python Package Index (PyPI) package and is accessible via BitBucket as well². spiops is also open to contribution from external users. Fig.1 provides a Jupyter notebook-based example that outlines the usage of spiops

3.1 adcsng a pipeline to process auxiliary data

SPICE Kernel Datasets of missions in operations (Mars-Express and ExoMars2016) are regularly updated in missions with new predicted and reconstructed trajectory and attitude information - usually provided by the mission's flight dynamics team- and with Housekeeping Telemetry that provides information of moveable parts of the S/C or the science payload [2]. With these data time-varying kernels are generated (SPKs, CKs and SCLKs) with an automatic processing pipeline: the Auxiliary Data Conversion System next generation (adcsng). adcsng is made available to the ESA missions as a Python Package.

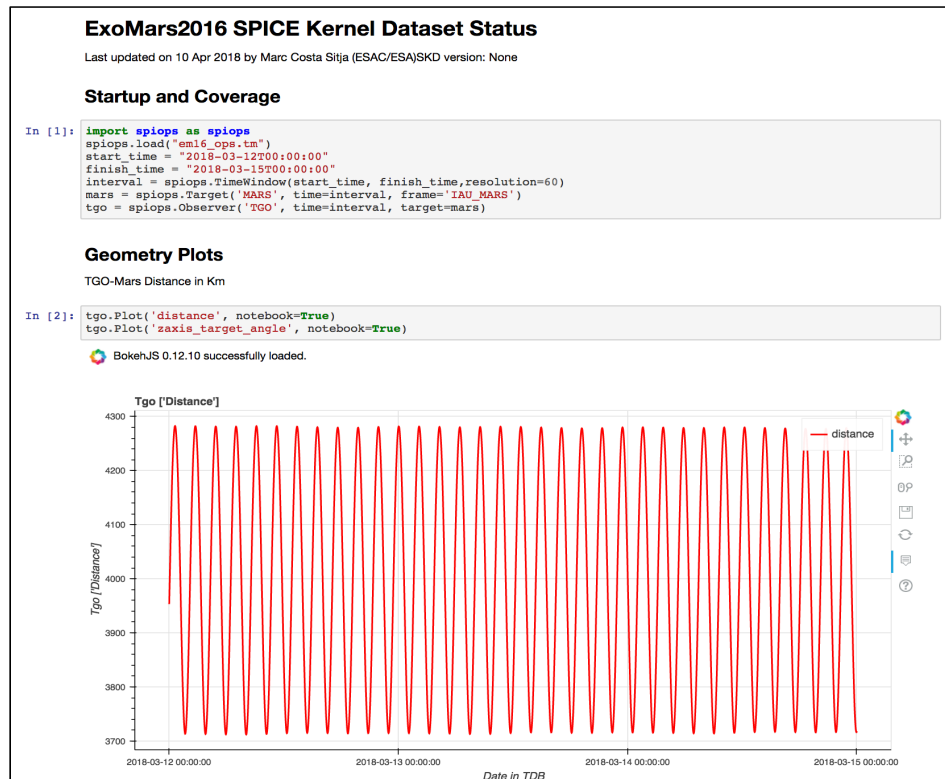


Figure 1 Jupyter notebook snippet outlining the usage of spiops

² <https://repos.cosmos.esa.int/socci/projects/SPICE/repos/spiops>

3.2 spispy and spival more Python packages for SPICE

Although these package is not open to contributions, ESS is also developing Python packages which in combination with adcsng and spiops will provide to the ESA SPICE users a web-based quick-look of a complete SKD.

In order to validate the SKD, to report the validation and to be used as a quick-look analysis spival, a private Python package has been to developed. spival features:

- Validation of the TVK-updated SKD after an execution of the Auxiliary Data Production Pipeline.
- Output of a Jupyter Notebook with a report of different geometry and S/C structures status:
 - S/C-Target Distance/Altitude
 - Sub-S/C point on Target
 - Boresight of interest angle w.r.t. Sub-S/C vector (e.g.: Offset from Nadir Pointing)
 - HGA Antenna Phase Center angle w.r.t. Earth
 - Solar Arrays Angles
 - Solar Aspect Angles for S/C Panels
 - S/C Groundtrack on target
 - ... and many more (open to suggestions)

In order to generate the reports spival heavily uses spiops. This reporting also provides information about the coverage and applicability of the given SKD³.

Using Cosmographia has the main drawback that the user needs to install it locally, sometimes a quick-look of a given mission 3D geometry context is of interest. Following that need we developed the private Python package spispy. spispy allows you to, in the shape of a Web app and by providing a time and a mission:

- Obtain a snapshot and the Cosmographia configuration of the 3D context of a given sensor that has a Field of View (FoV) defined in SPICE or a S/C reference frame direction.
- Obtain a snapshot of the trajectory of the S/C around a given body.
- Extend WebGeocalc functionalities with additional APIs available as a web-app

References

- [1] Acton C., Ancillary data services of NASA's Navigation and Ancillary Information Facility (1996), Planet. And Space Sci., 44, 65-70.
- [2] Costa M., SPICE for ESA Planetary Missions: geometry and visualization support to studies, operations and data analysis, this conference.

³Reports will be made available:
spice.esac.esa.int/status

An Integrated Software Environment to Improve the Photogrammetric Control Process for Planetary Mapping

Kenneth L. Edmundson (1), B.A. Archinal (1), J.C. Backer (1), T.L. Becker (2), K.L. Berry (1), C.R. Combs (1), D.A. Cook (1), A.C. Goins (1), I.R. Humphrey (1), J.A. Mapel (1), C.A. Neubauer (1), A.C. Paquette (1), M.R. Shepherd (1), S.C. Sides (1), E.D. Smith (1), S.G. Stapleton (1), T.L. Sucharski (1), L.A. Weller (1), and T.J. Wilson (1). (1) Astrogeology Science Center, U.S. Geological Survey, Flagstaff, AZ, USA (kedmundson@usgs.gov), (2) Lunar & Planetary Laboratory, University of Arizona, Tucson, AZ, USA.

Abstract

The Integrated Software for Imagers and Spectrometers (ISIS3) is developed and maintained by the U.S. Geological Survey Astrogeology Science Center (ASC) for the cartographic and scientific analysis of planetary image data [1]. The rigorous photogrammetric control of planetary images is a key ISIS3 capability, up to now requiring many standalone applications in a process that can be error-prone, inefficient, and costly. The ASC is developing in ISIS3 an *Integrated Photogrammetric Control Environment* (IPCE) offering a seamless, efficient, more intuitive and automated approach by integrating all aspects of the process in one environment [2].

1. Introduction

The quality of digital image mosaics (DIMs) and elevation models (DEMs)—and geologic maps using such products as basemaps—depends greatly upon accurate sensor position and pointing parameters. Spacecraft ephemeris and attitude data provide initial estimates for these parameters. Uncertainty in these data propagate to errors in mapping products (Figure 1). To minimize errors, images are controlled photogrammetrically. Overlapping images are registered to one another by measuring common features (tie points). Images may be tied to the ground

by measuring features identifiable on base maps or DEMs (control points). Image measurements are input to the least-squares bundle adjustment (BA) which generates improved sensor position and pointing parameters and tie and control point coordinates [4]. In practice the workflow is complicated and the tasks complex. One measures images; bundle adjusts; analyzes results; fixes errors; adds/removes data and/or measurements; fine-tunes settings; re-measures; re-adjusts; and iterates as necessary. Developing intuitive, user friendly software for photogrammetric control is not trivial.

2. IPCE

IPCE simplifies data management with the ability to save and restore project data and settings. Multiple, integrated views of data and processing results (Figure 2) have streamlined previously time-consuming tasks (e.g. creating, deleting, and editing points). The BA can be performed any number of times with results for each run available for examination via statistical and graphical analysis tools. Adjusted image position and pointing for each run are in the form of ISIS3 detached labels that can be applied to the original image data for map projection and mosaicking. Note that the image data itself is not duplicated.

3. The ISIS3 Bundle Adjustment

The ISIS3 BA is implemented in IPCE and as a standalone application (*jigsaw* [5]). In IPCE it runs in a separate thread from the main interface, so the user can continue to work. Images from different sensor types can be adjusted together and weighted appropriately. We can solve for target body parameters (e.g. pole position, spin rate, mean radius and/or semi-axes) and have applied this in processing a global network of Enceladus consisting of Cassini ISS images [6]. We now represent position and pointing of images from time dependent sensors (e.g. line scanners, radar) with piecewise continuous

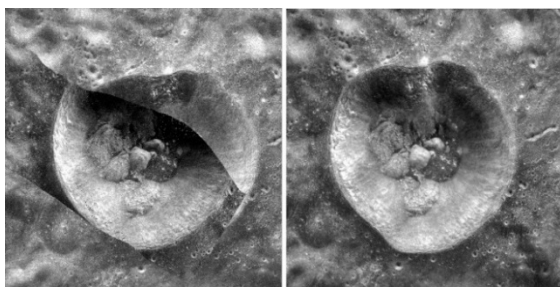


Figure 1: Uncontrolled & controlled mosaics of LRO Mini-RF radar images of the 20 km lunar crater Hermite A (87.94°N, 308.98°E), showing improvement in registration from >3 km to <30 m pixel scale (adapted from [3]).

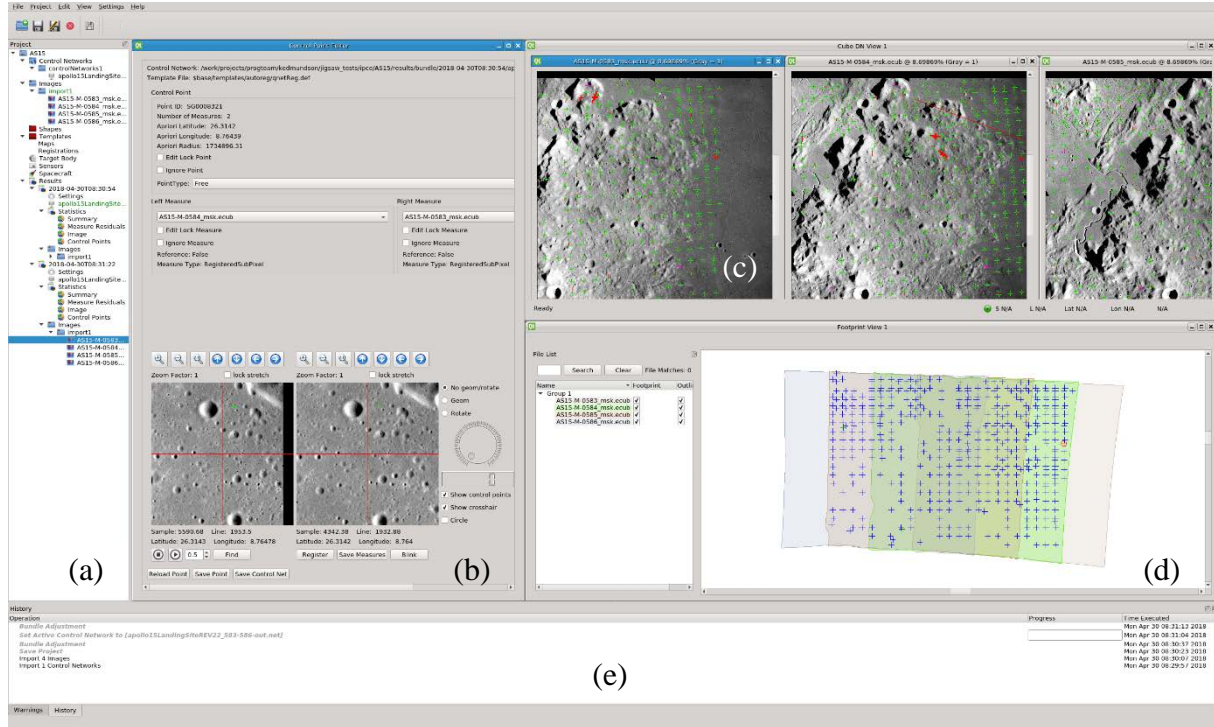


Figure 2: IPCE interface with (a) *project tree*, (b) *control point editor*, (c) *image display* (image measurements and residuals overlaid), (d) *image footprint view* (control points overlaid), and (e) *history and warnings* windows.

polynomials. Previously, position and pointing were modeled as single polynomial functions of time. Low-order polynomials cannot accurately represent complex spacecraft motions induced by, e.g. thruster firings, other instruments, or anomalous events. Higher-order polynomials could be used but can cause instability in the BA. In the piecewise polynomial approach, images are divided into segments represented by low-order polynomials [7]. We are currently implementing the rigorous combined adjustment of laser altimeter (LA) and image data in the BA (e.g. [8]). This will enable 1) the generation of improved sensor models, image position and pointing, and LA data sets; and 2) production of higher quality and accuracy digital terrain models that will facilitate landing site mapping, providing a greater margin of safety for future surface operations.

4. Upcoming Work

Plans include 1) improved automated image matching (e.g. [9]); 2) more analysis/visualization tools; 3) monitoring of control network state as edits occur; and 4) output of updated NAIF position/pointing kernels [10]. BA plans include self-calibration, free network adjustment [11], imposing conditions between sensors, variance component

estimation [12], improved outlier detection, sequential estimation, and solving for body libration.

Acknowledgements

Funding is provided by a NASA-USGS Interagency Agreement.

References

- [1] Sides, S., et al.: *LPS XLVIII*, #2739, 2017.
- [2] Edmundson, K.L., et al.: *LPS XLVI*, #1454, 2015.
- [3] Kirk, R.L., et al.: *LPS XLIV*, #2920, 2013.
- [4] Brown, D.C.: A Solution to the General Problem of Multiple Station Analytical Stereo Triangulation. *RCA Data Reduction Technical Report #43*, 1958.
- [5] Edmundson, K.L. et al.: *ISPRS Annals*, 1-4, 203-208, 2012.
- [6] Becker, T.L., et al.: *LPS XLVII*, #2342, 2016.
- [7] Poli, D.: Dissertation #15894, ETH Zurich, 2005.
- [8] Yoon, J. and Shan, J.: *Photogramm. Eng. Remote Sensing*, 71(10), 1179-1186, 2005.
- [9] Becker, K.B., et al.: *LPS XLVII*, #2959, 2016.
- [10] Acton, C.H., et al.: *Planet. Space Sci.*, 44(1), pp. 65-70, 1996.
- [11] Blaha, G.: *Bull. Géodésique*, 56(3), 209-219, 1982.
- [12] Koch, K-R.: *Parameter Estimation and Hypothesis Testing in Linear Models*, Springer-Verlag Berlin Heidelberg, 1988.

Analysis and global mapping of statistical parameters of Mercury relief characteristics

Anastasia Zharkova (1,2), Alexander Kokhanov (1) and Maria Kolenkina (1)

(1) Moscow State University of Geodesy and Cartography (MIIGAik), MIIGAik Extraterrestrial laboratory, Moscow, Russia, (2) Moscow State University Sternberg Astronomical Institute, Moscow, Russia (a_zharkova@miigaik.ru)

Abstract

Our work focuses on calculation of statistical parameters of relief characteristics for the whole Mercury surface, based on the newest DEMs. Also we concentrate on automation of geomorphological classification and mapping.

1. Introduction

The MESSENGER mission in 2011-2015 gives us an opportunity to gain new knowledge about Mercury which is still the least explored planet of the terrestrial group. The study of the relief characteristics by thematic mapping helps to identify common patterns in planetary relief and reveal hidden details. Calculations of Mercury statistical parameters were performed before according to the laser altimetry obtained by MESSENGER [1]. Because of the large eccentricity of the orbit, the altimeter provided measurements only for the northern hemisphere of the planet. Now our possibilities have expanded, because we are analyzing and mapping Mercury surface by new global and local DEMs.

2. Data and Methods

In our work for morphometric calculations we use the newest high resolution DEMs obtained based on photogrammetric processing of MESSENGER stereo images:

- the first global Mercury DEM with the resolution 665 m/pixel [2];
- DEMs on Mercury quadrangles with resolution ~222 m/pixel [3].

Depending on the tasks, the statistical parameters of planetary relief are calculated in different ways. For the purposes of our study we mostly use two techniques:

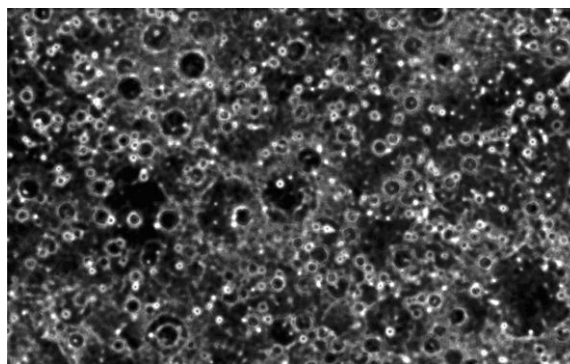
- Interquartile range of the second derivative of heights. For this method we use a previously developed tool integrated into the ArcGIS software [4]. Interquartile range gives the average notion about planetary relief, but at the same time it points to geological age of some features and shows old hidden structures that are not visible on images.

- Relative topographic position (RTP). For this method topographic position of each pixel is identified with respect to its local neighborhood [5]. Results of calculations are useful for identifying types of landscapes, prevailing geomorphological processes and defining boundaries of surface types.

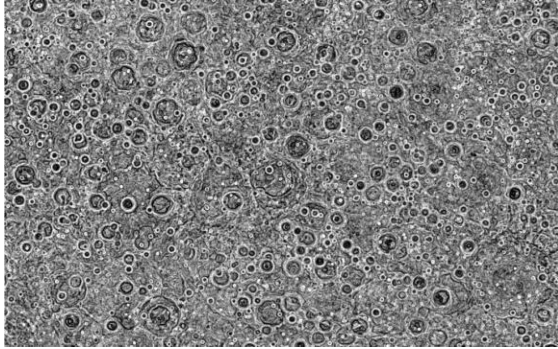
3. Main results

Using the global DEM with resolution of 665 m/pixel we have preliminarily calculated the statistical characteristics of entire Mercury by interquartile range method [6]. Then the relative topographic position was calculated.

For testing the automated geomorphologic zoning by calculations and classification of statistical parameters, the DEM of the site H-6 (Kuiper) was selected (Fig. 1 a,b).



a) Topographic roughness (on the basis of 32 km)



b) Relative topographic position (calculated in a 30-pixel window)

Figure 1: Calculations of statistical parameters of H-6 quadrangle (Kuiper) of Mercury based on detailed DEM (222 m/pixel): dark areas – smooth surface, bright – rough.

We used method of interquartile range of the second derivative of heights to find boundary values between different forms of macrorelief.

Figure 2 below shows an example of preliminary automated geomorphologic classification based on computed topographic roughness. We aimed to achieve high coherence between our suggested values of roughness for smooth plains and previously known boundaries of this type of Mercury relief form [7]. Obtained results showed good agreement.

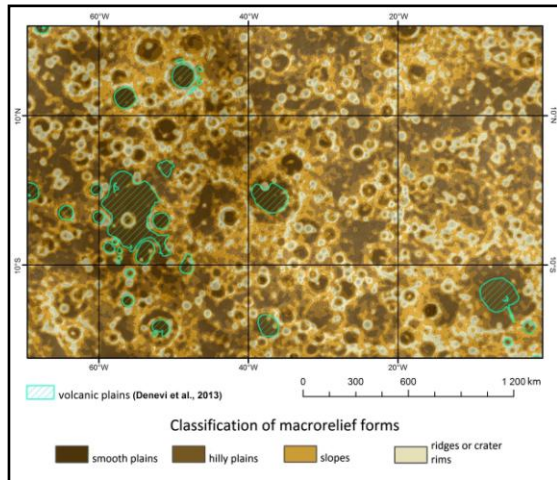


Figure 2: Trial classification of relief forms based on roughness values on H-6 quadrangle (Kuiper), green shaded areas correspond to the volcanic plains [12]

4. Verification of zoning

We used morphometric measurements of small craters (less than 1 kilometer in diameter) for additional verification of zoning results, because distribution of such craters depends on the type of surface.

Our analysis of about 1400 images, received by MESSENGER narrow-angle camera, showed that small craters with flat floors are mostly confined to Mercury's smooth plains (Table 1).

Table 1: Number and percentage of images with flat-floored craters within and outside geologically young smooth plains

	Images surveyed	Of them, with flat floored craters	Percentage
Within smooth plains	641	202	31.5%
Outside smooth plains	768	113	14.7%
Total	1409	315	22.4%

5. Summary and Conclusions

We are working on creation of the first global morphological map of Mercury, for which an automated classification of relief forms will be developed.

In the future, we plan to use the relative topographic position method more deeply. We hope that the combination of different methods will give us the opportunity to create the most complete classification of Mercury relief forms.

Such results can be used to process the data of the future European mission BepiColombo (2018).

Acknowledgements

This research was supported by Russian Foundation for Basic Research (RFBR), project № 18-35-00334.

References

- [1] Kreslavsky, M.A., Head, J.W., Neumann, G.A., Zuber, M.T., Smith, D.E.: Kilometer-Scale Topographic Roughness of Mercury: Correlation with Geologic Features and Units, *Geophysical research letters*, Vol. 4, Issue 23, pp. 8245-8251, 2014.
- [2] Becker, K.J., Robinson, M.S., Becker, T.L., Weller, L.A., Edmundson, K.L. Neumann, G.A., Perry, M.E., Solomon, S.C.: First Global Digital Elevation Model of Mercury, 47th Lunar and Planetary conference, The Woodlands, Texas, March 21-25, Abstract # 1903, 2016.
- [3] Preusker, F., Oberst, J., Stark, A., Matz, K-D., Gwinner, K., Roatsch, T.: High-Resolution Topography from MESSENGER Orbital Stereo Imaging – The Southern hemisphere, *EPSC Abstracts*, Vol. 11, EPSC2017-591, 2017.
- [4] Kokhanov, A.A., Bystrov, A.Y., Kreslavsky, M.A., Matveev, E.V., Karachevtseva, I.P.: Automation of morphometric measurements for planetary surface analysis and cartography, In *Int. Arch. Photogramm. Remote Sens. Spatial Inf. Sci.*, XLI-B4, p. 431-433, 2016, doi: 10.5194/isprs-archives-XLI-B4-431-2016.
- [5] Jenness, J. Topographic Position Index (TPI) v 1.2, Jenness Enterprises, 2006, http://www.jennessent.com/downloads/TPI_Documentation_online.pdf
- [6] Zharkova, A.Yu., Karachevtseva, I.P., Zubarev, A.E., Brusnikin, E.S., Kokhanov, A.A., Kreslavskiy, M.A.: Issledovanie poverhnosti Merkuriya kartograficheskimi metodami s ispol'zovaniem noveysih topograficheskikh dannyh, poluchennyh na osnove obrabotki izobrazheniy KA MESSENGER (The study of Mercury's surface by cartography methods based on the newest topographic data derived from MESSENGER image processing), *Sovremennye problemy distantsionnogo zondirovaniya Zemli iz kosmosa* (Current problems in remote sensing of the Earth from space), Vol.13, №5, pp. 265-274, 2016 http://d33.infospace.ru/d33_conf/sb2016t5/265-274.pdf, (in Russian).
- [7] Denevi, B.W., Ernst, C.M., Meyer, H.M., Robinson, M.S., Murchie, S.L., Whitten, J.L., Head, J.W., Watters, Th.R., Solomon, S.C., Ostrach, L.R., Chapman, C.R., Byrne, P.K., Klimczak, Ch., Peplowski, P.N.: The distribution and origin of smooth plains on Mercury, *Journal of Geophysical Research*, Vol. 118, Issue 5, pp. 891–907, 2013, doi: 10.1002/jgre.20075.

Crater size-frequency distribution measurements with CSFD Tools

Christian Riedel (1), Gregory Michael (1), Thomas Kneissl (1), Csilla Orgel (1), Harald Hiesinger (2) and Carolyn H. van der Bogert (2)

(1) Institute of Geological Sciences, Freie Universität Berlin, Germany, (2) Institut für Planetologie, Westfälische Wilhelms-Universität Münster, Germany (christian.riedel@fu-berlin.de)

Abstract

The analysis of crater size-frequency distributions (CSFDs) is a widely used technique to date and investigate planetary surface processes. For areas of high crater density, there are new geometric corrections that consider the effects of crater obliteration and subsequent recratering while measuring CSFDs. The new corrections require computationally intensive modifications of polygon geometries with respect to a curved planetary surface. Thus, in order to efficiently implement the new approaches in a software tool, we developed CSFD Tools, an application to conduct CSFD measurements from shapefiles. Our tool supports 64 bit and multi-core data processing and uses workarounds for the geodesic modification of polygon data. As a result, the new geometric corrections can be applied through a software tool.

1. Introduction

Absolute and relative ages of planetary surfaces have long been determined by statistical analyses of crater size-frequency distributions (CSFDs) [1,2]. The CSFD of a given surface unit is obtained by the application of CSFD measurement techniques. Such techniques describe which craters are included in the process and which reference area is assigned to each crater. There are two well-established techniques, traditional crater counting (TCC) and buffered crater counting (BCC) [3-5], and two new geometric corrections, non-sparseness correction (NSC) and buffered non-sparseness correction (BNSC) [6,7]. The new NSC and BNSC approaches are applied to consider the effect of crater obliteration by larger impact craters.

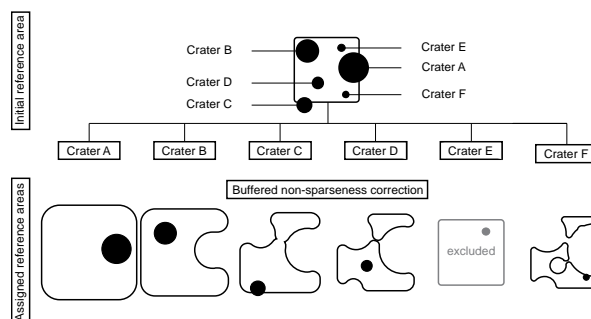


Figure 1: Assigned reference areas for six craters A-F during BNSC.

2. Review of the BNSC approach

The elimination of small craters through a larger impact crater can affect the shape of the CSFD and lead to variations when compared to observed crater formation rates [6]. To consider this effect when CSFD measurements are applied, larger craters plus their surrounding ejecta blankets are excluded from the reference area in the BNSC approach. The radius of a crater that is currently under investigation is used to buffer the remaining area (Figure 1). This implies that on densely cratered surfaces, small impact craters are only counted on areas which were unaffected by crater obliteration and subsequent recratering.

3. Implementation

We developed CSFD Tools to implement the new geometric corrections in a software tool that allows 64 bit and multi-core data processing. The tool uses open geospatial libraries to conduct GIS operations. However, current open geospatial libraries only allow geospatial operations on a two-dimensional Cartesian plane. Since impact craters are investigated on a curved planetary surface, this would lead to inaccurate results when CSFD measurements are

applied. To this end, we implemented a number of approaches for geodesic polygon modifications and measurements. This includes the geodesic buffering of polygons, geodesic measurements of area size, distance and azimuth on a biaxial ellipsoid as well as the automatic handling of Date Line intersections.

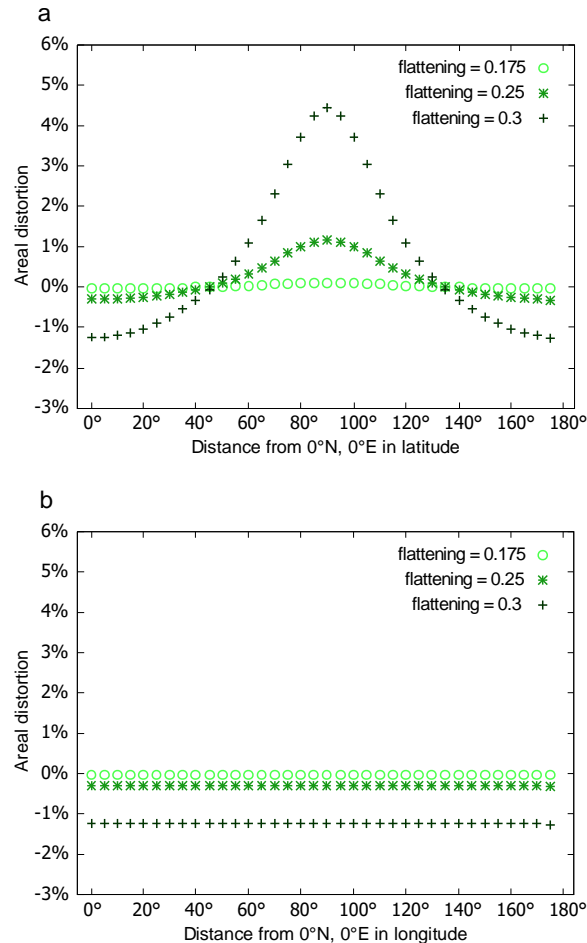


Figure 2: Distortion of area measurements in LAEA projection with growing eccentricity of the reference body. Measurements were conducted along the central meridian (Fig. 2a) and the equator (Fig. 2b).

4. Accuracy

The implemented methods for the consideration of a curved planetary surface include geodesic measurements of distance and azimuth as well as area measurements using Lambert azimuthal equal area projection (LAEA). The implemented geodesic measurements are accurate within 0.000015" on the reference body that is used [8]. To assess the accuracy of area measurements, we applied Tissot indicatrices [9] of a fixed size and investigated the

area distortion depending on its location and the eccentricity of the planetary reference body (Fig. 2). We found that distortions increase with growing distance from the equator and increasing eccentricity of the reference body. We consider the implemented methods valid for CSFD measurements on planetary bodies that can be approximated by a biaxial ellipsoid with a flattening of 0.3 or lower with a precision of better than 5%.

5. Conclusions

CSFD Tools is available as an executable Windows application and does not require any further software installations. The tool supports 64 bit and multi-core data processing and uses two input shapefiles for CSFD measurements. The procedure is independent from the attributes of the shapefiles. Accordingly, the digitization of reference area and impact craters can be conducted in any Desktop GIS. The data processing results in an SCC text file for further statistical analysis in the Craterstats software.

Acknowledgements

This work was supported by the German Research Foundation (DFG) SFB TRR-170 "Late Accretion onto Terrestrial Planets", Project A3.

References

- [1] Öpik, E. J.: The Lunar Surface as an Impact Counter, *Mon. Notices Royal Astron. Soc.*, Vol. 120, pp. 404-411, 1960.
- [2] Baldwin, R. B.: Lunar crater counts, *Astron. J.*, Vol. 69, pp. 377-392, 1964.
- [3] Kneissl, T., van Gasselt, S., and Neukum, G.: Map-projection-independent crater size-frequency determination in GIS environments – New software tool for ArcGIS, *Planet. Space Sci.*, Vol. 59, pp. 1243-1254, 2011.
- [4] Tanaka, K. L.: A new time-saving crater-count technique with application to narrow features, *NASA Technical Memorandum 85127*, pp. 123-125, 1982.
- [5] Fassett, C. I. and Head, J. W.: The timing of martian valley network activity: Constraints from buffered crater counting, *Icarus*, Vol. 195, pp. 61-89, 2008.
- [6] Kneissl, T., Michael, G. G., and Schmedemann, N.: Treatment of non-sparse cratering in planetary surface dating, *Icarus*, Vol. 277, pp. 187-195, 2016.
- [7] Orgel, C., Michael, G. G., Fassett, C. I. et al.: Ancient bombardment of the inner solar system - Reinvestigation of the 'fingerprints' of different impactor populations on the lunar surface, *J. Geophys. Res.: Planets*, Vol. 123, pp. 1-15, 2018.
- [8] Vincenty, T.: Direct and inverse solutions of geodesics on the ellipsoid with application of nested equations, *Survey Review*, Vol. 23, pp. 88-93, 1975.
- [9] Snyder, J. P.: Map projections – A working manual. U.S. Government Printing Office, 1987.

Datasets Fusion Techniques as the tool for analyzing the crustal properties of terrestrial and icy bodies to address their formation and geologic evolution in the Solar System

Piero D’Incecco (1), Edgard Rivera-Valentín (2)

(1) Arctic Planetary Science Institute, Berlin, Germany (piero.dincecco@planetaryscience.de), (2) Lunar and Planetary Institute, Universities Space Research Association, Houston, TX, USA (rivera-valentin@lpi.usra.edu)

Abstract

Multiple new space missions are now providing an increasing amount of data with improved quality to meet the challenges of Solar System exploration. Here, we propose the use of GIS methodologies for exploiting such remotely sensed data in order to perform a parallel investigation of the crustal properties of terrestrial and icy bodies. We name these procedures as “Datasets Fusion Techniques” (DFTs).

So far, we have successfully tested the use of DFTs on two rather different planetary environments, Mercury and Venus.

1. Successful DFTs tests

1.1 DFTs on Mercury

The MESSENGER MDIS and MASCS datasets have been combined to identify the eventual presence of horizontal and vertical compositional heterogeneities in the shallow crust of the planet. Impact deposits can in fact preserve and display the compositional heterogeneities occurring within the crust and the mantle of the planet [1]. A number of units have been defined on the basis of geologic criteria, retrieving all MASCS observations contained within each of these units from millions of globally distributed observations [2]. In this way, geologic interpretation was combined with spectral information [3,4]. On Mercury, the DFTs were applied both on a local scale (i.e., Figs. 1, 2) and on a global scale, extending this analysis to 121 impact craters uniformly distributed over the surface of the planet.

The results from the local and global scale investigations confirm that the geologic context and spectral characteristics of some impact deposits actually indicate the occurrence of vertical and

horizontal compositional heterogeneities in the shallow crust of Mercury [3,4]. The identification of such compositional diversities also allowed us to reconstruct the pre-impact local stratigraphy beneath two impact craters.

1.2 DFTs on Venus

1. We applied the DFTs on Venus combining Magellan SAR and the Venus Express VIRTIS datasets. The eastern flank of Idunn Mons, Imbr Regio’s large volcano, was identified by VIRTIS as one of the regions with relatively high values of thermal emissivity at 1 μm wavelength [5]. The main goal was to identify location and extent of the sources of such anomalies, thus the lava flows responsible for the relatively high emissivity observed by VIRTIS over the eastern flank of Idunn Mons. In this case, DFTs were performed iterating the geologic mapping made over Magellan radar images of the same area with modeling of the blurring caused by the scattering of the 1 μm radiation in the atmosphere. We tested eight different configurations (Fig. 3) [6].

Results show that the best-matching configuration is assigning high values of emissivity to the Idunn Mons’ flank lava flows.

2. DFTs and future missions

The automated application of DFTs for global scale study of the characteristics of the shallow crust of Mercury involved the simultaneous use of more than 4 million spectra, with an evident stress for the hardware components. The SQL spatial queries so far developed acted lightening the weight of the data processing on the hardware components; however, future missions [i.e., 7] may constitute a challenge in terms of Database Management System and data processing.

In conclusion, the future perspective of DFTs applications can be summarized with the following key points:

- Improving the synergy between the different constituents of DFTs, managing in the best way the interactions between hardware, OS, GIS software, SQL spatial queries and database. This can be achieved by continuously monitoring the data processing time.
- Applying the DFTs to other cases of study to exploit the full potential of these methodologies for the investigation of the mantle and crustal properties of other bodies of the Solar System, such as Venus, Mars, the Moon or the icy moons of Saturn.

3. Figures

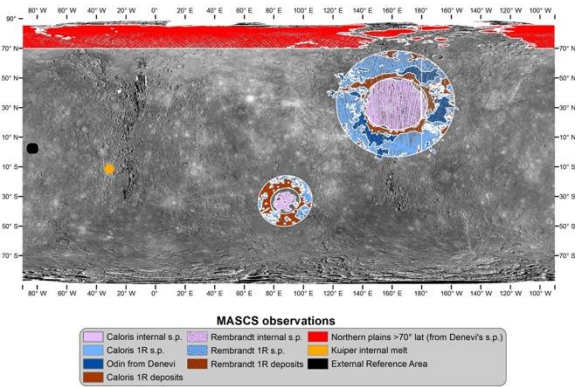


Figure 1 – MASCS spectral observations falling within a number of units, defined for Rembrandt and Caloris basins, and for the northern plains.

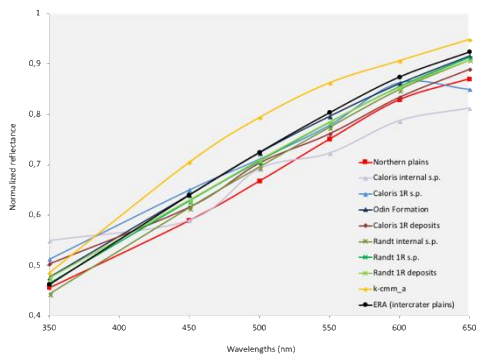


Figure 2 – Spectra extracted from the units in Fig. 1.

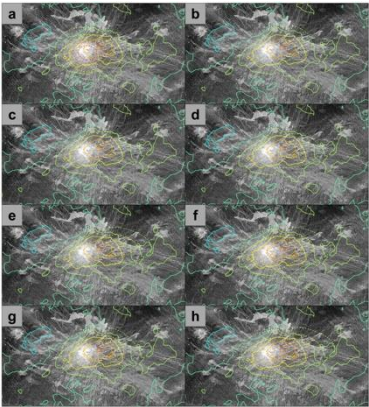


Figure 3 - Overlay between the 1 μ m thermal emissivity as observed by VIRTIS (continuous lines) and the thermal emissivity as resulting from the eight simulations (dashed lines)

References

- [1] Rivera-Valentin, E. G. and Barr, A. C., 2014. Estimating the Size of Late Veneer Impactors from Impact-induced Mixing on Mercury. *The Astrophysical Journal Letters*, Volume 782, Issue 1, article id. L8, 6 pp., doi:10.1088/2041-8205/782/1/L8.
- [2] Izenberg, N.R., et al., 2014. The low-iron, reduced surface of Mercury as seen in spectral reflectance by MESSENGER. *Icarus* 228, pp. 364-374, <http://dx.doi.org/10.1016/j.icarus.2013.10.023>.
- [3] D’Incecco, P., et al., 2015. Shallow crustal composition of Mercury as revealed by spectral properties and geological units of two impact craters. *Planetary and Space Science*, Volume 119, p. 250-263, doi:10.1016/j.pss.2015.10.007.
- [4] D’Incecco, P., et al., 2016a. A geologically supervised spectral analysis of 121 globally distributed impact craters as a tool for identifying vertical and horizontal heterogeneities in the composition of the shallow crust of Mercury. *Planetary and Space Science*, Volume 132, p. 32-56, doi:10.1016/j.pss.2016.08.004.
- [5] Smrekar, S. E., et al., 2010. Recent hot-spot volcanism from VIRTIS Emissivity data. *Science*, 328, 5978, 605-608.
- [6] D’Incecco, P., et al., 2016b. Idunn Mons on Venus: location and extent of recently active lava flows. *Planetary and Space Science*, ISSN 0032-0633, <http://dx.doi.org/10.1016/j.pss.2016.12.002>.
- [7] Glaze, L., et al., 2017. VICI: Venus In situ Composition Investigation, #EPSC2017-346.

A summary report on 3D imaging software, data and their distribution from the EU FP-7 iMars project

Jan-Peter Muller, Yu Tao, Panagiotis Sidiropoulos and the iMars consortium

Imaging group, Mullard Space Science Laboratory, University College London, Holmbury St Mary, RH5 6NT, UK
(j.muller@ucl.ac.uk)

Abstract

In this paper, we summarise the main achievements from the completed EU FP-7 iMars project (<http://www.i-mars.eu>) including the distribution of open access data products and software.

1. Background and Context

Almost fifty years have elapsed since the NASA Mariner 4 spacecraft first took the pictures of the Martian surface. Over that time, the resolution and quality of these images has improved from tens of kilometres down to 25 cm. Over the intervening ≈ 50 years, many areas on Mars have been repeatedly imaged as each new science team has “re-invented the wheel” and gone back to the same places highlighted by these early images. Historically, the driver for these scientific studies has been the “hunt for water” but more recently, there is an increasing interest in studying different dynamic phenomena associated with the motion of dust and surface-atmospheric interactions. The revolution in planetary surface observations, especially in 3D imaging of surface shape, has led to the ability to be able to overlay different time epochs back to the mid 1970's, to examine time-varying changes, such as the recent discovery on Mars of mass (e.g. boulder) movement, tracking inter-annual seasonal changes and looking for fresh impact craters from meteoritic strikes. As our exploration of surface changes proceeded we determined that the polar regions had some of the most significant surface changes and so a great deal of emphasis was changed to focus on these regions.

Within the iMars project, we wanted to mitigate the deleterious effects of increasing knowledge and accuracy of where the spacecraft was located in its orbit and where the cameras were pointing to allow fully automated computer algorithms to eliminate the impact of these errors and provide co-registered image products so we can playback any area on Mars, which had repeat coverage. Of course, in many cases no change can be observed, however surprisingly the surface is much more dynamic than at first thought

particularly with regard to very dynamic phenomena like dust devils. When the technology developed by iMars is rolled out across the planet in future it is very likely that new discoveries will be made. For polar regions, the number of repeat views is significant as well as for regions such as the putative and actual landing sites, Vallis Marineris, the Tharsis volcanic region and other regions repeatedly imaged on the boundary of the so-called dichotomy. Little, if any, information is available on the variability of the Martian surface, although the annual and seasonal changes associated with the polar cap expansion and contraction and the rapid spread of dust storms has been relatively well monitored in the past. However, the Martian surface is undergoing frequent changes from our observations of just 3% of the surface so we do not yet know what we can fully expect to find.

2. Method

The iMars project focused on developing tools and value-added datasets to massively increase the exploitation of space-based data from NASA and ESA Mars mission imaging data and derived 3D data beyond the PI teams. iMars has added significant value by creating more complete and fused 3D models of the surface from multi-resolution co-registered stereo with all 3D imaging products co-registered to a global reference system derived from laser altimetry. iMars has also shown how these 3D models can be employed to create a set of co-registered imaging data through time, permitting a much more comprehensive interpretation of the Martian surface to be made.

Emphasis was placed on the co-registration of multiple datasets from different space agencies and orbiting platforms around Mars and their synergistic use to discover what surface changes have occurred since NASA's Viking Orbiter spacecraft first went into orbit around Mars more than forty years ago.

iMars brought together the best expertise in Europe for the processing of Martian orbital data within a single environment for handling, visualising and interpreting these data. The ESA Mars Express High Resolution Camera (HRSC) provided the 3D mapping products

used as base data (for around 50% of the surface), where possible. When CTX stereo products are also available over the same areas as HRSC (for around 20% of the surface) then the CTX products can be co-registered with HRSC and CTX 3D mapping products can then be employed as the base data for higher resolution images such as MOC-NA and HiRISE. A Co-registered Ames Stereo Pipeline using Gotcha Optimization (CASP-GO; *Tao et al, PSS, 2018*) was developed for large-scale production of CTX 3D mapping products and small area production of HiRISE products. Some 5,300 CTX stereo products have been processed using cloud computing provided by Microsoft Azure® covering about 20% of the Martian surface. In iMars, standards were set for the production and dissemination of HRSC mosaiced products, which are easier to utilize for co-registration than individual strips and have better internal geometry. A fully automated Auto-Coregistration and Orthorectification (ACRO; *Sidiropoulos & Muller, 2015, 2017*) system was developed to operate on a linux cluster without any manual intervention. Around 15,000 NASA images (out of the $\approx 400,000$ acquired with resolution of $\leq 100\text{m}$) were processed using the ACRO system covering around 4% of the surface. New HRSC 3D mapping products (Putri, this conference) were produced for the South Polar Residual Cap area and we are working on applying the same approach to the North Polar cap in collaboration with another iMars partner. ACRO products have therefore been processed as well as multi-resolution DTMs from CTX and HiRISE. A large portion of the 3D mapping products have been analysed qualitatively by visual inspection and the ACRO processing includes calculating internal quality metrics, which are used to flag bad products.

An automated data mining algorithm was developed to find scene fragments where single or multiple instances of change are detected. This used supervised classification initially with planetary science labelled inputs but will in the near future employ mass public participation from a shortly-to-be-launched citizen science programme under the auspices of Zooniverse. A great deal of effort was placed on determining the optimum Human Factors for incentivising and motivating such participants. Each additional set of a minimum of 10 identifications and notations will be further employed to improve the classification (standing it is believed at around 50%) and the data mining applied to new areas by non-EU funded students at Masters and PhD level.

3. Results and future work

All of these new products are viewable through an OGC-compliant webGIS developed at FUB which is hosted at MSSL (<http://www.i-mars.eu/web-gis>; Walter et al., JGR/ESS, 2018). This includes tools for viewing temporal sequences of co-registered ORIs over the same area. This allows experts and members of the public to examine different parts of the planet for changes as well as perform geomorphological and geological research.

In parallel, a citizen science project at Nottingham University has defined training samples for classification of change features and for verification of change. Scientific use cases include new craters & slope streaks.

Distribution of the iMars products will take place through ESA PSA and NASA PDS in PDS4 standards. The CASP-GO software will be released through the NASA Ames ASP Github.

The iMars base data can be used by the ESA ExoMars Trace Gas Orbiter 2016 and subsequent ESA missions to provide the necessary inputs for selection of a future landing site for the ESA ExoMars 2020 rover and for any Mars Sample Return missions in the 2020s. It will greatly extend the use of the archived data by providing mapped and co-registered products.

Acknowledgements

Part of the research leading to these results has received partial funding from the European Union's Seventh Framework Programme (FP7/2007-2013) under iMars grant agreement n° 607379 and MSSL STFC Consolidated grant no. ST/K000977/1.

References

- [1] Tao, Y., J.-P. Muller, et al., (2018) Planetary and Space Science. Vol. 154, pp.30-58.
- [2] Sidiropoulos, P., & J.-P. Muller, IEEE Trans. Geosci. Rem. Sens., doi: 10.1109/TGRS.2017.2734693.
- [3] Walter, S.H.G., J.-P. Muller, P. Sidiropoulos, Y. Tao, et al, (2018) The iMars web GIS – an interactive online mapping tool for the spatio-temporal visualization of topography data and dynamic time-series of single image layers. JGR/ESS special issue: Planetary Mapping: Methods, Tools for Scientific Analysis and Exploration.

Geodata workflow for the AMADEE-18 Mars analog mission

Nina Sejkora (1,2), Sebastian Sams (2,3) and Gernot Groemer (2) for the AMADEE-18 Mission Team
(1) Technical University of Graz, Austria, (2) Austrian Space Forum, Innsbruck, Austria, (3) University of Innsbruck, Innsbruck, Austria (nina.sejkora@oewf.org)

Abstract

During the AMADEE-18 Mars analog field campaign, a human-robotic Mars mission was simulated in the Dhofar region in Oman, where a field crew was supported by a Mission Support Center (MSC) in near-real time. Instrument workflows, pilot data analysis was emulated in a workflow as it is to be expected for future a human-robotic Mars mission. We report on an innovative geodata workflow, ensuring an efficient mapping and deployment interaction of geographical information between the field crew and the MSC.

1. Introduction

AMADEE-18 was an international Mars analog simulation mission of the Austrian Space Forum (OeWF), in partnership with the Oman Astronomical Society. The mission took place in the Dhofar region in Oman in February 2018, including 19 experiments looking into engineering, geoscience and human factors research for future human-robotic Mars missions (Fig.1).

A highly trained field crew, including 7 analog astronauts with high-fidelity spacesuit simulators were directed in real-time by a control center on "Mars" during Extravehicular Activity (EVA) and through time-delayed communications by the Mission Support Center on "Earth" in Austria.

1.1 Exploration cascade

The experiment selection and deployment modalities were choreographed according to an "exploration cascade", representing a logical data acquisition, transfer and interpretation workflow as a basis for the operational planning. The concept included carefully designed flight plans of the field crew, data transfer of instrument data in near-real time (with a 10min

signal delay), a pilot interpretation of the data by the principal investigators and a subsequent influencing of the flight plan, connecting both scientific needs with spaceflight-typical workflows.



Figure 1: Kepler-Station for the AMADEE-18 Mars simulation in Oman.

1.2. Mars-analog geopositioning

As a global positioning system will not be available for the first human Mars mission, relative positioning techniques including horizon profile or inertial navigation, complemented with triangulation based upon signal travel times might allow for navigational capabilities comparable to terrestrial GPS. The spacesuit simulators utilized GPS signals to mimic those projected navigation capabilities.

2. Geodata management

2.1. Geodata sources and preparation

The base layer data upon which subsequent analysis and planning was founded, were the following: an optical aerial image with a resolution of 0.5 m and a digital elevation model (DEM) with a resolution of 5 m, both acquired via the Oman National Survey Authority. Additionally, as the AMADEE-15 mission [2] showed the importance of not only spatial, but also temporal resolution, data by Planet [5] was used, which has a high update rate at a resolution of 3 m.

Before mission start, the DEM was analyzed to classify the region w.r.t. inclines. High inclines, which may be exhausting or even dangerous to climb, were avoided. Also the experiment teams had access to the data to identify areas of interest, and communicate them for in-mission traverse planning.

During the mission itself, the Flight Planning (FP) team developed the daily traverse plans. Those plans specified the locations where to perform scientific experiments, and traverses in between. The FP team was assisted by the Remote Science Support (RSS) team and external PIs with respect to the scientific value of potential target sites. Traverse plans also need to consider operational constraints (see e.g. [3]), such as communication infrastructure and flight rules for extra-vehicular activities. Hence, eg, the coverage obtained by a specific setup of WLAN antennas was modeled based on the DEM with a viewshed analysis.

2.2. Geodata deployment workflow

Traverse planning and geodata analysis efforts in previous missions showed shortcomings when using stand-alone software like Google Earth without a sophisticated workflow for managing and distributing the data [4]. Furthermore, the MARS2013 mission [1] showed the necessity for a system to assist the analog astronauts to orient themselves at the area of operations [4]. This requires to efficiently make the output of the planning process available to devices deployed in the field.

During AMADEE-18 we implemented a workflow for handling geodata to allow efficient collaborative editing and sharing of data between teams. Data was stored on a central server and made available to clients using open standards as defined by the Open Geospatial Consortium (OGC). This allows to access the data via any standard compliant software. The workflow relied heavily on the use of transactional capabilities of the Web Feature Service (WFS) protocol, allowing to directly edit data on the server from within the client software. To allow sharing a specific version of a data set, read-only copies of the current state could be created.

We used GeoServer¹ as server software, as it provides an open-source and OGC compliant implementation of the required protocols and

supports a wide range of data formats. Management may be automated using a REST API, which was utilized to implement the functionality for copying layers and preparing templates for individual teams.

Whenever a team created a versioned snapshot of their work, the data was transferred automatically to another server instance in the field. The process also implemented the time-delayed transfer as required in the context of the analog simulation. Base layer data was prepared beforehand and deployed on the field server. Clients in the field could then retrieve all published data locally. This included the space suit simulator, allowing the automated display of the most recent data on the Head-Up-Display.

Positions of the analog astronauts were recorded automatically by the space suit simulator using GPS. Current data was transmitted continuously with a time-delay to the MSC via the internal telemetry system, providing “live” tracking. All logged positions were also transferred after each EVA via other established communication channels developed during previous missions. Data was then imported into the server and made available to all teams as input for their next plans and record of actual experiment locations. This allowed integration with already existing workflows whilst still utilizing the capabilities of the new system

References

- [1] Groemer, G., Soucek A., Frischauf N., et al.: The MARS2013 Mars analog mission. *Astrobiology* Vol.14 (5), pp. 360-376, 2014.
- [2] Groemer, G., Losiak, A., Soucek, A., et al.: The AMADEE-15 Mars simulation. *Acta Astronautica* Vol. 129, pp. 277-290, 2016.
- [3] Hörz, F., Lofgren, G. E., Gruener, J. E., et. al.: The traverse planning process for D-RATS 2010. *Acta Astronautica*, Vol. 90 (2), pp. 254-267, 2013.
- [4] Losiak, A., Gołębiewska, I., Orgel, C., et al.: Remote science support during MARS2013: testing a map-based system of data processing and utilization for future long-duration planetary missions. *Astrobiology* Vol. 14 (5), pp. 417-430, 2014.
- [5] Planet Team (2017). Planet Application Program Interface: In *Space for Life on Earth*. San Francisco, CA. <https://api.planet.com>.

¹ <http://geoserver.org>

Automated feature detection and tracking of RSLs at Valles Marineris through super-resolution restoration and deep learning using HiRISE images and 3D terrain models

Y. Tao and J.-P. Muller

Imaging group, Mullard Space Science Laboratory, University College London, Holmbury St Mary, RH5 6NT, UK

(yu.tao@ucl.ac.uk; j.muller@ucl.ac.uk)

Abstract

In this paper, we demonstrate novel computer vision and deep learning techniques on detecting and tracking of Recurring Slope Lineae (RSL) features in the Valles Marineris area using repeat-pass HiRISE images and Digital Terrain Models (DTMs).

1. Introduction

Studying the transport and formation processes on the Martian surface requires accurate measurements of dynamic features and the underlying 3D static surface. Tracking of such dynamic features has never been achieved automatically before due to the fact that detection and classification methods usually require a static reference frame and do not perform well when the feature itself is changing all the time. In this work, we propose a new approach to detect and track the dynamic features by extracting the “static part” of the Martian surface through super-resolution restoration (SRR) using repeat-pass HiRISE observations.

This study focuses on RSLs which are metre-to decametre-wide dark streaks found on steep slopes, which grow during the warmest times of the year, fade during the cooler periods and reappear again (but not necessarily in exactly the same place). The origin of these features is controversial, with some authors suggesting they are formed by water or brine and others suggesting they are completely dry processes. The implications of each of these formation mechanisms is fundamental to constraining Mars’ water budget and habitability.

We selected Valles Marineris, where the highest concentration of RSLs is found on Mars. In the longer term, we aim to provide the first regional map of RSL occurrence, with associated growth rates, timings (including inter-annual variability) and topographic information (including slopes and orientation). In this report, we present the first stage of this study which is using SRR and deep learning techniques to automatically detect and track the RSL features,

derive robust measurements, and their associated 3D information.

2. Method

Previously within the EU FP-7 Planetary Robotics Vision Data Exploitation (PRoViDE) project (<http://provide-space.eu>), we developed a novel super-resolution algorithm called GPT-SRR [3] to restore distorted features from multi-angle observations using advanced features and an area matcher, Gotcha [2] and regularization approaches, achieving a factor of up to 5x enhancement in resolution [4][6].

More recently funded by the UKSA CEOI (SuperRes-EO), we have further developed the SRR system using advanced machine learning algorithms, applied to EO data. The new SRR system is based on the Mutual shape adapted Features [1] from Accelerated Segment Test (O-FAST) [8] and Convolutional Neural Network (CNN) [9] feature matching, the Support Vector Machine (SVM) and Graph Cut (GC) based shadow modelling and removal [10], and the Generative Adversarial Network (GAN) [11] deep learning based super-resolution refinement. The new MSA-FAST-CNN-GPT-GAN (MAGiGAN) [12] system not only retrieves subpixel information from multi-angle distorted features from the original GPT algorithm, but also uses the loss calculated from feature maps of the GAN network to replace the pixel wise difference based content loss of the original GPT algorithm to retrieve high texture detail.

Due to the ability of the SRR technique to extract super-resolution for static features, we are able to restore matched (unchanged) features and meanwhile automatically track the unmatched (dynamic) pixels to characterize and measure the “change”. Combining with a CNN based classifier, the detected dynamic changes can be further classified to known dynamic features, such as RSLs.

In parallel, within the completed EU FP-7 iMars project (<http://www.i-mars.eu>), we have developed a

fully automated multi-resolution DTM processing chain for CTX and HiRISE stereo-pairs, called the Co-registration Ames Stereo Pipeline (ASP) Gotcha Optimised (CASP-GO) [5], based on the open source NASA ASP [13] [14], with Gotcha sub-pixel refinement [1] and a unique tie-point based multi-resolution image co-registration system [7]. The CASP-GO system guarantees global geo-referencing congruence with respect to the aerographic coordinate system defined by HRSC, level-4 products and thence to the MOLA, providing much higher resolution stereo derived DTMs.

At the next stage, by adding 3D information from repeat DTMs produced from multiple overlapping stereo-pairs, we are able to restore the unchanged surface also in 3D as SRR requires multiple angle views as inputs. This allows us to overlay tracked dynamic features onto the reconstructed “original” surface, providing a much more comprehensive interpretation of the surface formation processes in 3D.

3. Results

We report on detailed results from a study of one of the RSL sites (centre coordinates: 41.6°S, 202.3°E) in the Palikir Crater, with 8 repeat-pass 25cm HiRISE images from which a 5cm SRR image using GPT-SRR was produced. The SRR image shows the restored static surface without any dynamic features. By tracking the unmatched features from the original HiRISE images, we are able to initially mask out the dynamic features (i.e. RSLs) on the static surface.

Recently, supported by the UKSA-Aurora programme, we are exploiting the CASP-GO system to generate new very high resolution 3D products from HiRISE (see locations in Figure 1) over 40 locations in Valles Marineris using our in-house imaging cluster and the Amazon® AWS cloud computing resources. In this work, we show the latest results of automated RSL detection and tracking using the new MAGiGAN SRR system, a CNN based feature classification system, and CASP-GO.

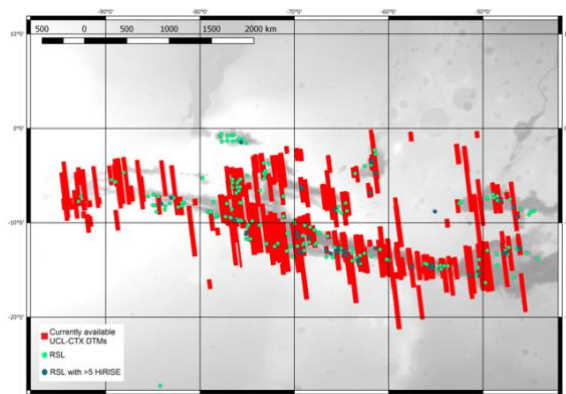


Figure 1 Map of the Valles Marineris region showing a MOLA DTM as the background image with footprints of the available CASP-GO CTX DTMs (in red), the locations of all HiRISE images (in green) and of RSLs identified by [15] and those with 5 or more HiRISE images.

Acknowledgements

The research leading to these results is receiving funding from the UKSA Aurora programme (2018-2021). Part of the research leading to these results has received partial funding from the European Union’s Seventh Framework Programme (FP7/2007-2013) under iMars grant agreement n° 607379 and MSSL STFC Consolidated grant no. ST/K000977/1. The authors would like to thank Susan Conway for her science inputs.

References

- [1] Tao, Y., J.-P. Muller, W. Poole (2016) *Icarus*, vol 280, p139-157. [2] Shin, D. and J.-P. Muller (2012) *Pattern Recognition*, 45(10): p.3795 -3809. [3] Tao, Y. and J.-P. Muller (2015) *Planetary and Space Science* [4] Tao, Y., J.-P. Muller (2016) *ISPRS 2016 Commission IV, WG IV/8*. [5] Tao, Y., J.-P. Muller, et al., (2018) *Planetary and Space Science*. Vol. 154, pp.30-58. [6] Bridges, J.C., J. Clemmet, D. Pullan, M. Croon, M.R. Sims, J.-P. Muller, Y. Tao, S.-T. Xiong, A. D. Putri, T. Parker, S.M.R. Turner, J.M. Pillinger, (2017) *Royal Society Open Science*, 4(10), p.170785. [7] Sidiropoulos, P., & J.-P. Muller, *IEEE Trans. Geosci. Rem. Sens.*, doi: 10.1109/TGRS.2017.2734693. [8] Rosten et al., *IEEE*, 2010 [9] Fischer et al., *CVPR*, 2014 [10] Qi et al., *CVPR*, 2011 [11] Ledig, *CVPR*, 2016 [12] Tao & Muller, 2018 in preparation [13] Moratto et al., 2010 [14] Broxton et al., 2008 [15] Stillman et al., 2017.

ACRI-ST: From data to science

Jeronimo Bernard-Salas, Nick Cox, Jean-Luc Vergely, Stéphane Ferron, Laurent Blanot, Lauriane Delaye, Véronique Bruniquel, Odile Hembise Fanton d'Andon
ACRI-ST, 06904 Sophia-Antipolis, France (nick.cox@acri-st.fr, jeronimo.bernard-salas@acri-st.fr)

Abstract

ACRI-ST is an independent SME (small and medium-sized enterprise) of the Space sector based in France, supplier of the space agencies, specialised in scientific research activities, engineering and operations. With a long-history and experience on Earth Observations, the company is currently expanding its involvement in Planetary Sciences and Astronomy. ACRI-ST works in close collaboration with national and European laboratories and has built long-term partnerships with academic research institutes and organizations to support the scientific community with the development of end-to-end instrument simulators, data processing chains, calibration and validation analyses, data archiving and distribution facilities, downstream services development and operations. In this contribution we will present ACRI-ST competences and its expertise with a focus on Space Sciences.

1. Introduction

ACRI-ST¹ is the “Space” company of the ACRI Group established in 1989, which addresses the whole chain of the Space sector from support to on-board instrument specifications and data ground segment development to operational services for end-users. The headquarters of ACRI-ST are located in Sophia-Antipolis. The company is present in France with two other establishments in Paris and Toulouse and a French subsidiary ARGANS-France in Brest and also in Sophia-Antipolis. The company has also an international presence through its subsidiaries in UK (ARGANS-UK), Luxemburg (adwaïsEO), Canada (ARCTUS) and Morocco (ACRI-EC).

ACRI-ST is a trusted supplier to space agencies (simulation of space-based sensors; calibration/validation activities, operational chains development; processing, archiving and mission

performance centres) and develops/operates environmental Copernicus-EU (Sentinel) services for end users. ACRI-ST offers solutions and decision-making support based on the study and modelling of physical and environmental phenomena, simulation and prototyping. It exercises research and training, more specifically ACRI-ST focuses on development, validation and operation of observation and modelling techniques or the inversion of data for science.

ACRI-ST plays thus a role in the whole chain (Figure 1), from sensors measurements specification to the production of relevant information to scientists, policy-makers, and economic stake-holders.

2. Expertise in the Space Segment

ACRI-ST is specialized in data calibration and validation, processing, archiving and distribution, as well as prototyping and engineering of data processors, data quality check systems, end-to-end sensors simulators. These competences can be grouped in 3 main areas:

- **Space domain sciences:** studies in support to Agencies and satellite manufacturers for new missions and sensors specifications; development of end-to-end instrument simulators for performance studies in preparation of the use of remote sensing data for environmental applications; prototyping of level 1 to 3 data processing algorithms; instrumental behaviour analysis; quality control and calibration/validation activities.
- **Systems and Software engineering:** operational chains development and handling of large data-volumes (near-real time processing, storage and distribution) in the context of “Big Data in Space”; development of Thematic Exploitation Platforms (TEPs) for analysis and exploitation of spatial missions.
- **Data Services:** archiving and processing services (reprocessing) of space missions, operating mission performance centres.

¹Website: www.acri-st.fr.

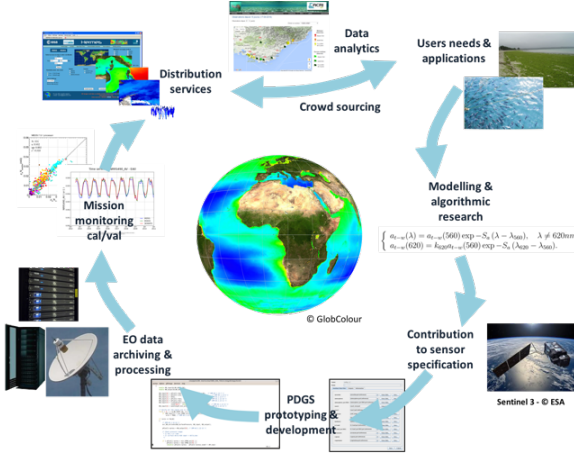


Figure 1: Example of the range of ACRI-ST competences and activities in Earth Observation.

3. Space Sciences Data Expertise

Several ACRI-ST R&D engineers have backgrounds (PhD) in astrophysics and planetary science. Through their involvement in numerous optical and infrared ground-based, airborne and space-based facilities for astrophysics and planetary science (e.g. AKARI, ALMA, GAIA, Gemini, Herschel, ISO, JWST, Mars Express, SOFIA, SPICA, SOHO, Spitzer, Venus Express, Very Large Telescope) there is a broad range of in-house experience and expertise in the Space Sciences.

ACRI-ST experts encompass a wide range of technical and scientific expertise in infrared, optical, and ultraviolet imaging and spectroscopy. Our engineers and scientists have experience among others, in data processing and analysis of (spectral)-imaging, time-series signal processing, development of optimal extraction algorithms, creating large astronomical data catalogues, source extraction and multi-survey cross-matching, image stitching and reconstruction (in accordance to astrometry), as well as data interpretation of interstellar gas and planetary atmospheres with radiative transfer models.

4. References in Space Science

ACRI-ST has used its technical expertise in Earth Observations for projects in the Space Sciences. For example, we have produced for ESAC, in partnership with LATMOS (Paris), SPICAM/SPICAV UV Level 2

data (reflectance and transmission spectra) and atmospheric composition parameters (trace gas abundances and aerosol properties) for Mars and Venus. These new data products will be publicly available from ESA's planetary science archive.

For the European Horizon-2020 project UPWARDS we have contributed to the (improved) retrieval of the vertical distribution of H₂O-vapour in Mars' atmosphere using a novel technique utilising spectral synergy between the near-infrared (NIR) and thermal-infrared (TIR) channels. ACRI-ST also provides expertise on inversion techniques to reconstruct the 3-dimensional distribution of interstellar dust (extinction) from colour-excess and distance (parallax) data for the French ANR project STILISM. ACRI-ST engineers provided operational support and contributed to the scientific exploitation of the SWAN instrument on-board SOHO; in particular regarding the estimation of the solar wind and its helio-latitudinal dependence. ACRI-ST has also a strong expertise in radiative transfer models for Earth applications, which led also to participating to the development of the Atmospheric Transmission for Astro database (TAPAS).

5. Research & Development

ACRI-ST R&D engineers in Space Sciences are also involved in research in a variety of topics in Space Sciences, such as planetary atmospheres, comets, evolution and production of dust and organic matter in interstellar and circumstellar environments, astrochemistry, star-formation, and stellar and galaxy evolution.

ACRI-ST works in close collaboration with national and European laboratories and has built long-term partnerships with academic research institutes and organizations. The company also funds master and PhD theses. ACRI-ST engineers/scientists continuously foster their links with the scientific community, attending scientific conferences and (co-)authoring scientific publications.

Photoscan DEMs from Apollo 15 Hasselblad Photographs

Madeleine Manheim, Robert Wagner, Susan Klem, and Mark Robinson
(1) School of Earth and Space Exploration, Arizona State University, USA (mmanheim@ser.asu.edu)

Abstract

Eighty 70 mm Hasselblad photos taken by Apollo 15 astronauts at EVA 3 stations 9A and 10 were used to create a 7.3 cm/px digital elevation model of an 800 m x 500 m section of Hadley Rille. Ground control was taken from an LROC NAC DTM. We present a production methodology and error analysis for this DEM, and use it to conduct preliminary block counts at a meter to sub-meter scale.

1. Introduction

Hasselblad 70 mm cameras were used to collect images of Hadley Rille and its vicinity during Apollo 15 surface operations. Astronauts took panoramic series of images at several locations, enabling the creation of digital elevation models (DEMs). The Agisoft Photoscan software can produce georeferenced DEMs and accurate orthophotos from sets of images without the need for *a priori* pointing information [1, 12, 16]. Thus, Apollo surface photography represents a resource for creating very high resolution models of the lunar surface.

Previous photogrammetric work on Apollo 70 mm surface photography largely focused on identifying camera positions, rather than creating orthomosaics [9, 13]. Recently, Hasselblad photographs from Apollo 17 were used with photogrammetry software to make a 3D model of a sample site in order to determine the sample's orientation [17]. In this work, we create a DEM and corresponding orthomosaic, georeference it to an overlapping LROC NAC DEM, and demonstrate its use for block size-frequency distribution (SFD) studies.

Finding correlation between meter and sub-meter block populations is essential for identifying the back-scattering effects of blocks in radar signals [8, 15]. Orbital observations can identify blocks at the meter scale; for example, LROC NAC DTMs are 50 cm/px at 50 km altitude, allowing confident measurements of rocks down to about 2.5 m in diameter. Handheld surface photography, once georeferenced, is a viable source for measuring blocks at sub-meter scales [6, 14]. Here, we introduce a new dataset using Apollo surface imagery that covers blocks in the 0.4 m to 3 m range.

2. DEM Production in Photoscan

We selected 187 70 mm Hasselblad photos that were taken during EVA 3 at stations 9A and 10. Of these, 157 were taken with a 500 mm focal length lens, and 30 with a 60 mm lens [2]. These photos were downloaded as JPGs from the Apollo Lunar Surface Journal, cropped by up to 2 pixels to produce consistent image dimensions [3], and imported into Photoscan. The software was able to align 80 of the photos (51 with the 500 mm lens and 29 with the 60 mm lens), producing a dense point cloud of 33,469,579 points and covering a 800 m x 500 m region on Hadley Rille's west side (Fig. 1).

We then added 5 ground control points chosen from an LROC NAC DTM covering the same area [NAC_DTM_APOLLO15, 10]. To work around Photoscan's inability to correctly project onto non-terrestrial surfaces, the coordinates for these points were selected as the map-projected x and y coordinates from the

LROC DEM, along with the elevation relative to the lunar ellipsoid [4]. The use of these coordinates implicitly aligned the xyz model produced by Photoscan to the coordinate reference system of the LROC NAC DTM.

From this georeferenced dense point cloud, we produced two DEMs at 7.3 cm/px, with and without interpolation across sparse regions of the dense point cloud. We then used Photoscan to project the images onto the interpolated DEM, producing a 7.3 cm/px orthomosaic (Fig. 1).

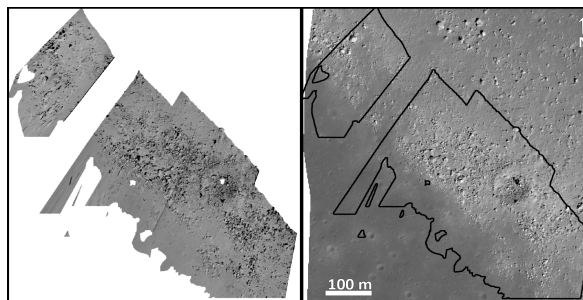


Figure 1: Comparison of orthomosaic from Photoscan (left) and LROC NAC orthophoto (right).

3. Quality Check

Qualitative comparison between the NAC DTM and the Photoscan DEM indicated minimal offsets or differences in scaling. A gnomon is visible in two of the aligned images, which were a stereo pair of a sample site and fortuitously had Hadley Rille in the background. This instrument has a rod that is gimbaled to remain vertical at all times. We added reference points to the model at the top and bottom of this rod to determine that the model's vertical axis is tilted by 1.1°. We attempted to use the gnomon to check the model's scale as well, as it has a known size [18]. However, we found the scale of the gnomon to be off by about an order of magnitude, unlike the rest of the model. This may be because the gnomon is ~2 m away from the camera, while the terrain covered by the DEM is 1.2 km away, and the stereo baseline between the two images is very small compared to the model size.

We ran the program *pc_align* from the AMES stereo pipeline to control the point cloud to the NAC DTM [11]. The resulting optimal shift for the point cloud was 0.03 m south, 1.99 m east, and 0.027 m down.

4. Block Counts

Using our 7.3 cm/px orthomosaic, we counted blocks in a region 100 m downslope by 67 m cross-slope. The downslope direction is roughly parallel to the camera's line of site, and thus rocks appear "smeared" in that direction (Fig 2). Removing regions that are interpolated in the DEM reduces this effect. Therefore, we counted only blocks whose boundaries lie primarily in the non-interpolated regions. Further, because the blocks were very dense in the measured region, blocks > 3 m were almost always too interpolated or obscured by other large blocks to be confidently measured.

Maximum diameter was measured for all the blocks in the region of interest with diameters < 3 m [5, 7]. The minimum reliably resolved block size was 0.36 m, or five times the native pixel scale. We followed [5] in computing slope of our cumulative block SFD. The 696 blocks counted were cumulatively binned in 0.1 m intervals and plotted on a log-log scale (Fig 3).

Previous lunar block studies have tended to fit a power law to block counts [5]. However, although our block SFD does level out at diameters < 0.6 m, the transition between populations fits an exponential model between 0.6 m and 2.6 m (Fig 3). Although our block analysis results are preliminary, they indicate that Apollo Hasselblad photographs can be used to evaluate how cumulative block SFDs change between meter and sub-meter block populations.

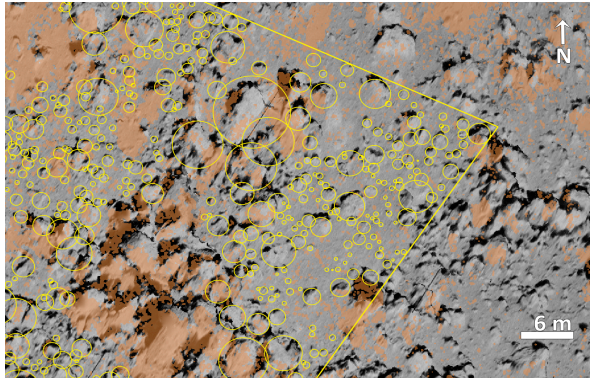


Figure 2: Portion of block counts in the Photoscan orthophoto. Counts are circled in yellow; interpolated regions of the orthomosaic are shown in orange.

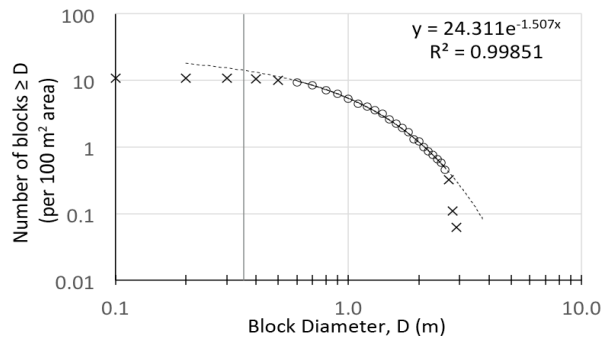


Figure 3: SFD of block counts for a 6,438 m² area in the Hadley Rille DEM. Data points used to produce the exponential fit are marked with circles; excluded data points are marked with Xs. The vertical grey line indicates 0.36 m, the lowest diameter that can be reliably resolved.

5. Discussion

The model produced by Photoscan performed well in both qualitative and quantitative evaluations, indicating that Apollo surface photography can be an accurate source of photogrammetric data at scales smaller than is possible from orbital images. These small scales can facilitate studies such as block size frequency distributions, as well as landing site and

traverse risk analysis. Photoscan's ability to create models without any *a priori* camera model or pointing information will allow for the creation of numerous models from other Apollo landing sites and other sources of surface photography.

References

- [1] <http://www.agisoft.com/>
- [2] Apollo 15 Index of 70 mm Photographs, 1972. Available at http://apollo.sese.asu.edu/SUPPORT_DATA/index.html.
- [3] Apollo Lunar Surface Journal, Apollo 15 (<https://www.hq.nasa.gov/alsj/a15/a15.html>).
- [4] Archinal, B. A. et al., *Celest. Mech. Dyn. Astron.*, Vol. 109 (2), pp. 101-135, 2011.
- [5] Cintala, M.J. and McBride, K. M., *NASA Tech. Mem.*, 1995.
- [6] Di, K. et al., *Planet. & Space Sci.*, Vol. 120, pp. 103-112, 2015.
- [7] Kneissl, T. et al., *Planet. & Space Sci.* Vol. 59, pp. 1243-1254, 2010.
- [8] Ghent, R. R. et al., *Icarus*, Vol. 273, pp. 182-195, 2016.
- [9] Haase, I. et al., *J. Geophys. Res. Planets*, Vol. 117, E12, 2012.
- [10] Henriksen, M. R. et al., *Icarus*, Vol. 283, pp. 122-137, 2017.
- [11] Intelligent Robotics Group, *The Ames Stereo Pipeline*, v. 2.5.3, 2017.
- [12] Ostwald, A. M. and Hurtado, J. M., *LPSC, The Woodlands, TX, Abstract #1787*, 2017.
- [13] Pustynski, V. V. and Jones, E. M., *J. Br. Interplanet. Soc.*, Vol. 67, pp. 390-398, 2010.
- [14] Shoemaker E. M. & Morris E. C., *Surveyor Project Final Report Part II*, pp. 86-102, 1968.
- [15] Spudis, P. D. et al., *J. Geophys. Res. Lett.*, Vol. 118, pp. 2016-2029, 2013.
- [16] Wagner, R. V. et al., *3rd Planetary Data Workshop*, Flagstaff, AZ, 2016.
- [17] Wells, R. A. et al., *LPSC, The Woodlands, TX, Abstract #1085*, 2018.
- [18] Wolfe, E.W. et al., *USGS Prof. Paper 1080*, 1981.